

# *4-D evolution of rift systems: Insights from scaled physical models*

**K. R. McClay, T. Dooley, P. Whitehouse, and M. Mills**

## **ABSTRACT**

The four dimensional (4-D) evolution of brittle fault systems in orthogonal, oblique, and offset rift systems has been simulated by scaled sandbox models using dry, cohesionless, fine-grained quartz sand. Extensional deformation in the models was controlled by the orientation and geometry of a zone of stretching at the base of the model. The results of these analog model studies are compared with natural examples of rift fault systems.

Rift basins produced by orthogonal and oblique rifting are defined by segmented border fault systems parallel to the rift axes and by intrarift fault systems that are subperpendicular to the extension direction. Segmentation of the rift margin increases with increase in obliquity of the rift axis, resulting in a consequent increase in displacement on intrarift fault systems. Offset rift models are characterized by highly segmented border faults and offset subbasins in the rift zone.

Along-strike displacement transfer in the model rifts occurred as a result of formation of two types of accommodation zones. High-relief, extension-parallel accommodation zones typically are found in 60° rifts and above left steps in offset rift systems. Changes in fault polarities in these accommodation zones were achieved by interlocking arrays of conjugate extensional faults. The second type of accommodation zone was generally oblique to the extension direction and consisted of conjugate fault arrays having rotated tips that bounded a low-relief oblique-slip zone or grabens. These typically are found in highly oblique rift systems (<45°) and above right steps in offset rift models.

## **INTRODUCTION**

Many natural rift systems display along-strike changes in extensional fault polarities and in offset grabens and depocenters along the rift axis (cf. Bally, 1981; Gibbs, 1983, 1984, 1987; Bosworth,

## **AUTHORS**

**K. R. McClay** ~ *Fault Dynamics Research Group, Geology Department, Royal Holloway University of London, Egham, Surrey, TW20 0EX, United Kingdom; ken@gl.rhul.ac.uk*

Ken McClay graduated with a B.Sc. (honors) degree from Adelaide University, Australia. He subsequently undertook an M.Sc. degree in structural geology and rock mechanics at Imperial College, London University, where in 1978 he also obtained a Ph.D. in structural geology. He was awarded a D.Sc. by Adelaide University, Australia, in 2000. He is BP Professor of Structural Geology and director of the Fault Dynamics Research Group at Royal Holloway University of London. His research involves the study of extensional thrust, strike-slip, and inversion terranes and their applications to hydrocarbon exploration. He publishes widely, consults, and offers short courses to industry.

**T. Dooley** ~ *Fault Dynamics Research Group, Geology Department, Royal Holloway University of London, Egham, Surrey, TW20 0EX, United Kingdom; t.dooley@gl.rhul.ac.uk*

Tim Dooley, a native of Waterford, Ireland, graduated with a B.A. (honors) degree (Mod.) from Trinity College Dublin, Ireland, in 1988. Subsequently, he undertook a Ph.D. in structural geology at Royal Holloway University of London. Since 1994 Tim has been a postdoctoral research assistant with the Fault Dynamics Research Group in the structural modeling laboratories at Royal Holloway. His current research interests include analog modeling of extensional, strike-slip, salt and shale, and compressional tectonics, as well as developing graphic and interactive techniques for the presentation of these data to students and industry.

**P. Whitehouse** ~ *Fault Dynamics Research Group, Geology Department, Royal Holloway University of London, Egham, Surrey, TW20 0EX, United Kingdom; p.whitehouse@gl.rhul.ac.uk*

Paul Whitehouse graduated from the University of Birmingham in 1996 with a B.Sc. degree in geology. In 1998, he completed an M.Sc. degree in basin evolution and dynamics at Royal Holloway University of London

Copyright ©2002. The American Association of Petroleum Geologists. All rights reserved.

Manuscript received May 26, 2001; revised manuscript received June 4, 2001; final acceptance January 2, 2002.

before joining the Fault Dynamics Research Group as a postgraduate research assistant. His recent research topics include analog modeling of three-dimensional extensional fault systems and analog modeling of doubly vergent thrust wedges. His current work concentrates on fault and fracture systems in extensional tectonic settings, incorporating analog modeling and field studies in the Gulf of Suez, Egypt.

**M. MILLS ~ Fault Dynamics Research Group,  
Geology Department, Royal Holloway  
University of London, Egham, Surrey, TW20  
OEX, United Kingdom**

Michelle Mills graduated from the University of Edinburgh in 1997 with a B.Sc. degree in geology, having spent her third year at the University of California, Santa Cruz. She spent a year as a voluntary worker before completing her M.Sc. degree in tectonics at Royal Holloway College in 1999. She currently works at Heriot-Watt University evaluating computer-aided learning software for engineering.

## ACKNOWLEDGEMENTS

This research was supported by the Natural Environment Research Council (NERC) ROPA Grant GR3/R9529. Additional support came from the Fault Dynamics Project (sponsored by ARCO British Limited, Petrobrás U.K. Ltd., BP Exploration, Conoco [United Kingdom] Limited, Mobil North Sea Limited, and Sun Oil Britain). McClay also gratefully acknowledges support from BP Exploration. Howard Moore and Mike Creager constructed the deformation apparatus. This article is Fault Dynamics Publication 101.

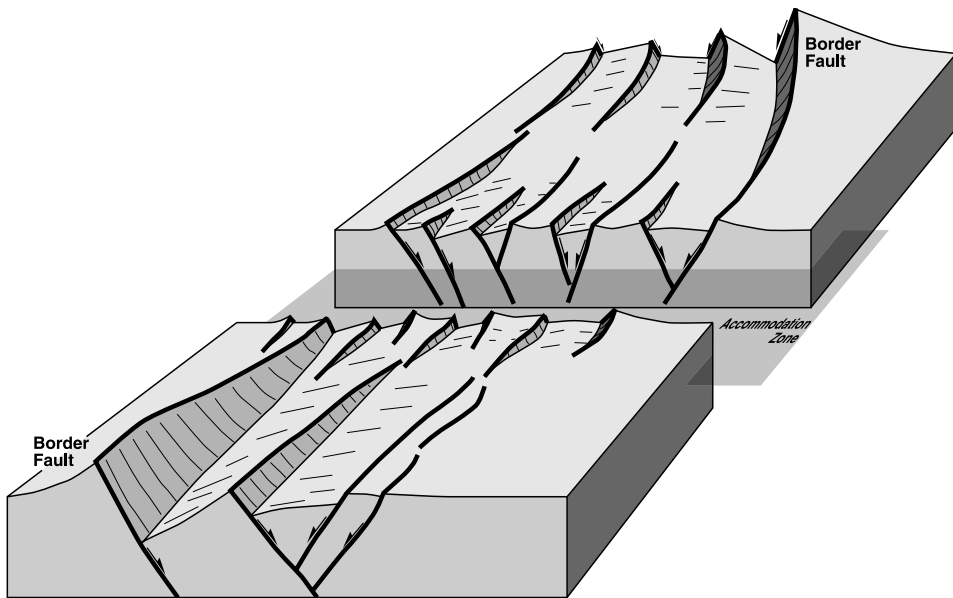
1985, 1994; Lister et al., 1986; Rosendahl et al., 1986; Etheridge et al., 1987; Rosendahl, 1987; Ebinger, 1989a, b; Morley et al., 1990, 1994; Nelson et al., 1992; Faulds and Varga, 1998). This segmentation in rift systems characteristically occurs every 50–150 km along the rift axis (Rosendahl et al., 1986; Patton et al., 1994; Hayward and Ebinger, 1996); increased extension and continental separation may ultimately lead to segmentation along conjugate passive margins (cf. Karner and Driscoll, 1999). Two end-member models (Figure 1) have been proposed to account for these changes in fault polarities and offset depocenters: (1) the hard-linked strike-slip or oblique-slip transfer fault model (cf. Bally, 1981; Gibbs, 1983, 1984; Lister et al., 1986) and (2) the soft-linked accommodation zone model of distributed faulting without distinct cross faults or transfer faults (cf. Bosworth, 1985, Rosendahl et al., 1986; Morley et al., 1990; Morley, 1994; Mousatova, 1997; Faulds and Varga, 1998). The detailed structure and kinematic evolution of these changes on rift polarities and on the development of accommodation zones, however, are poorly understood.

Scaled analog sandbox models have proved to be powerful tools for simulating the development of extensional structures in rift systems (e.g., Cloos, 1968; Horsfield, 1977, 1980; Faugere and Brun, 1984; Withjack and Jamison, 1986; Serra and Nelson, 1989; McClay, 1990a, b; Tron and Brun, 1991; McClay and White, 1995). This article summarizes the results of a new series of three-dimensional (3-D) sandbox models of orthogonal, oblique, and offset rift systems in which rift segmentation and discrete accommodation zones are well developed. These model results are compared with natural intracontinental rift systems.

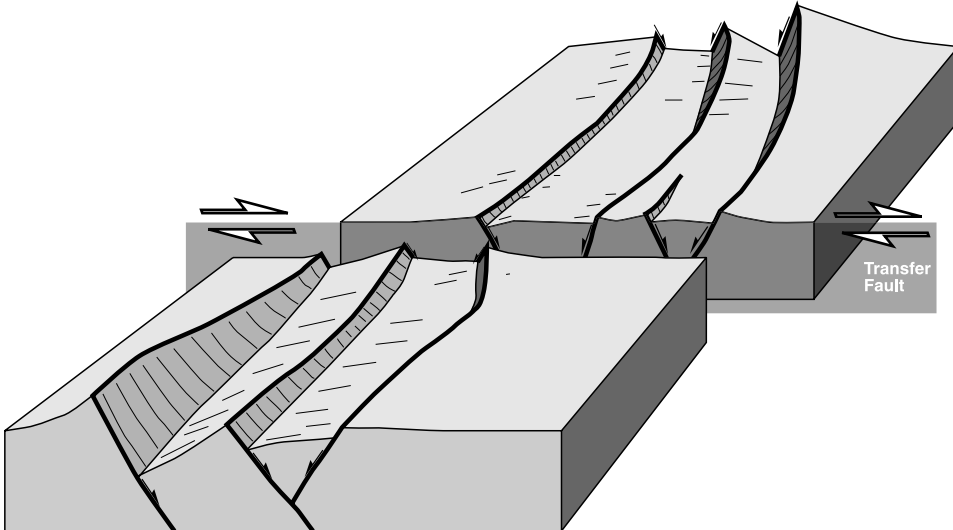
## ANALOG MODELING

### Experimental Method

The experiments were carried out in a deformation rig 120 × 60 × 7.5 cm in size (Figure 2). The models consisted of a 7.5 cm-thick sandpack formed by mechanically sieving 2–3 mm-thick layers of white and colored dry, quartz sand (average grain size 100 µm) on top of a basal detachment formed by a 10–15 cm-wide rubber sheet fixed between two aluminum end sheets. The rubber sheet was either parallel sided or offset by discrete basal transfer faults (Figure 2c). The baseplate axes were oriented at angles of from 90° (orthogonal) to 45° (oblique) to the extension direction. Deformation was achieved by moving both of the end walls with a motor-driven worm screw at a constant displacement rate of 4.16 × 10<sup>-3</sup> cm/sec (Figure 2). The models were extended in 0.25 cm increments to a maximum of 7.5 cm, measured orthogonally to the rift axis; the top surfaces were recorded by 35 mm photography. Oblique rift models were extended to a maximum of 10.65 cm parallel to the long axis of the deformation apparatus to



**a**



**b**

**Figure 1.** Conceptual models of displacement transfer in rift systems. (a) Synoptic model of a low-strain intracontinental rift with along-axis segmentation. Individual half grabens are separated by soft-linked accommodation zones formed by overlapping fault segments. (b) Synoptic model of hard-linked, strike-slip, rift transfer-fault system.

achieve the required 7.5 cm stretching of the rubber basesheet (Figure 2). After each 2 cm of deformation, the accommodation space was infilled with alternating layers of white and red sand to simulate synrift sedimentation. The quartz sand has a linear Navier-Coulomb behavior that has an angle of friction of 31° (McClay, 1990b). The models described in this article are scaled such that they simulate brittle deformation of a sedimentary sequence between 1 and 10 km in thickness (Figure 3) (cf. McClay, 1990a). The models for each baseplate geometry investigated were repeated at least twice to ensure reproducibility and to allow for both horizontal and vertical sectioning.

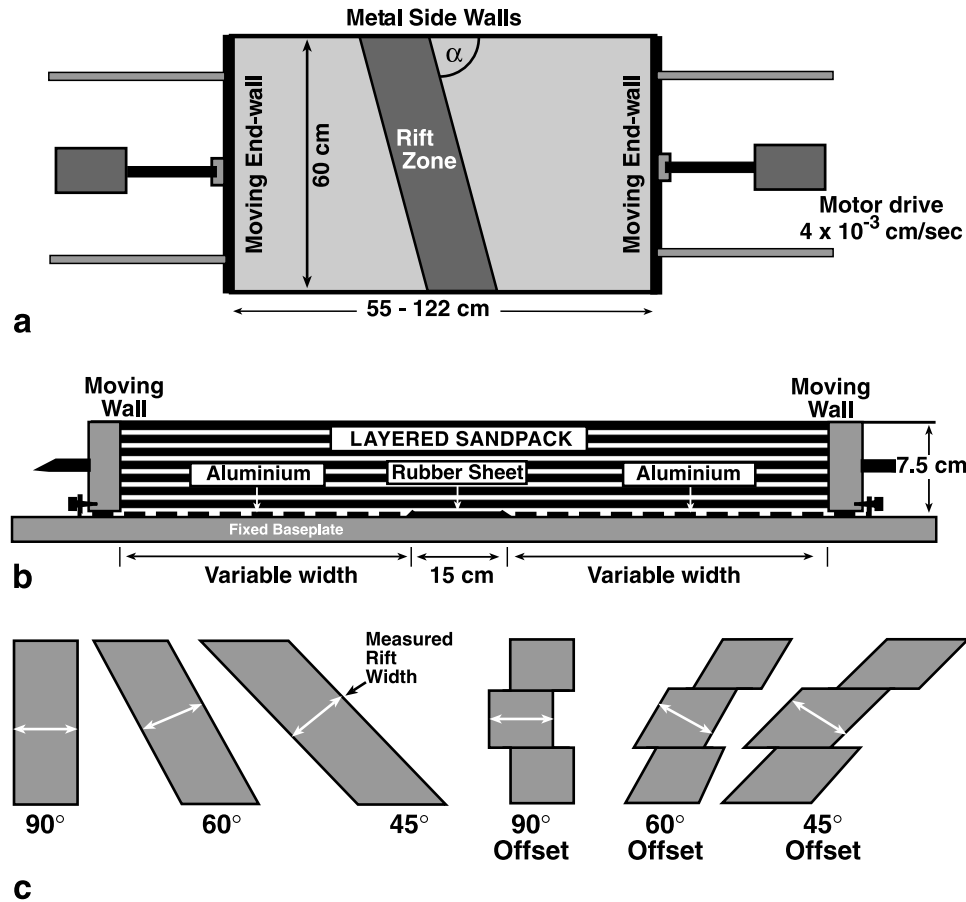
## Results

Representative results from orthogonal, oblique, and offset rift models are illustrated in Figures 4–9. Top photographs, line diagram interpretations, and serial vertical sections are presented for each example.

### Orthogonal Rift Models

In orthogonal rift models, where the underlying zone of basement stretching was oriented 90° to the extension direction, the early stages of deformation were characterized by long, linear, extensional faults that formed as a result of along-strike linkage of initially

**Figure 2.** Analog modeling rig. (a) Plan view showing baseplate orientation with respect to the extension direction. (b) Cross-section view of deformation rig. (c) Baseplate geometries used in this study: 90° (orthogonal models), 60°, 45° (oblique rifts and offset rifts).



smaller linear-fault segments (Figure 4a). Two long rift-border faults were well developed by 4 cm of extension, together with an intrarift fault system that defined a central horst block and two linear graben systems on each side of it (Figure 4a). Using increased extension to 50% stretching at the base of the model, individual extensional faults increased their displacement, and extension tended to focus inward to the centers of each graben system (Figure 4b). The line diagram of Figure 4c shows the dominant fault systems that have a characteristic switch in fault dip (polarity) across the model. All faults developed at high angles (near 90°) to the extension direction. Serial cross sections through the completed model show the symmetrical nature of the rift system, its cylindricity along strike, and grabens that developed adjacent to each border fault and the central horst block (Figure 4d). Individual faults show kinks along their traces (Figure 4a, b, c) where initially separate segments have linked. Overlap zones between like-dipping faults form relay ramps (Figure 4c), but no accommodation zones or strike-slip transfer faults were developed in these orthogonal rift models.

#### Oblique Rift Models

In contrast to the orthogonal rift models, oblique rift experiments were characterized by strongly segmented fault systems and offset-basin depocenters in the rift (Figures 5, 6). The 60° oblique model (Figure 5) initially developed arrays of intrarift fault systems oriented at high angles to the extension vector, and rift margins were formed by individual, en

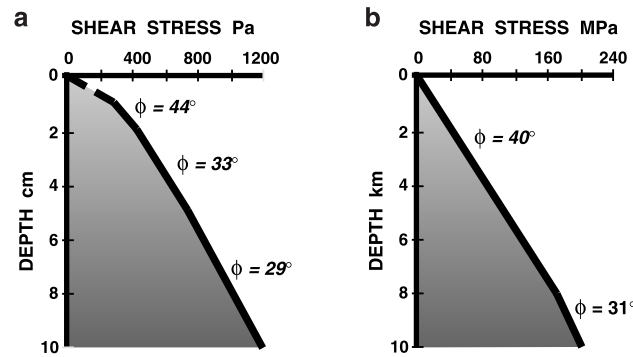


**Figure 3.** Scaling parameters for the simulation of brittle deformation of sedimentary rocks in the upper crust. (a) Detachment; (b) brittle-plastic transition.

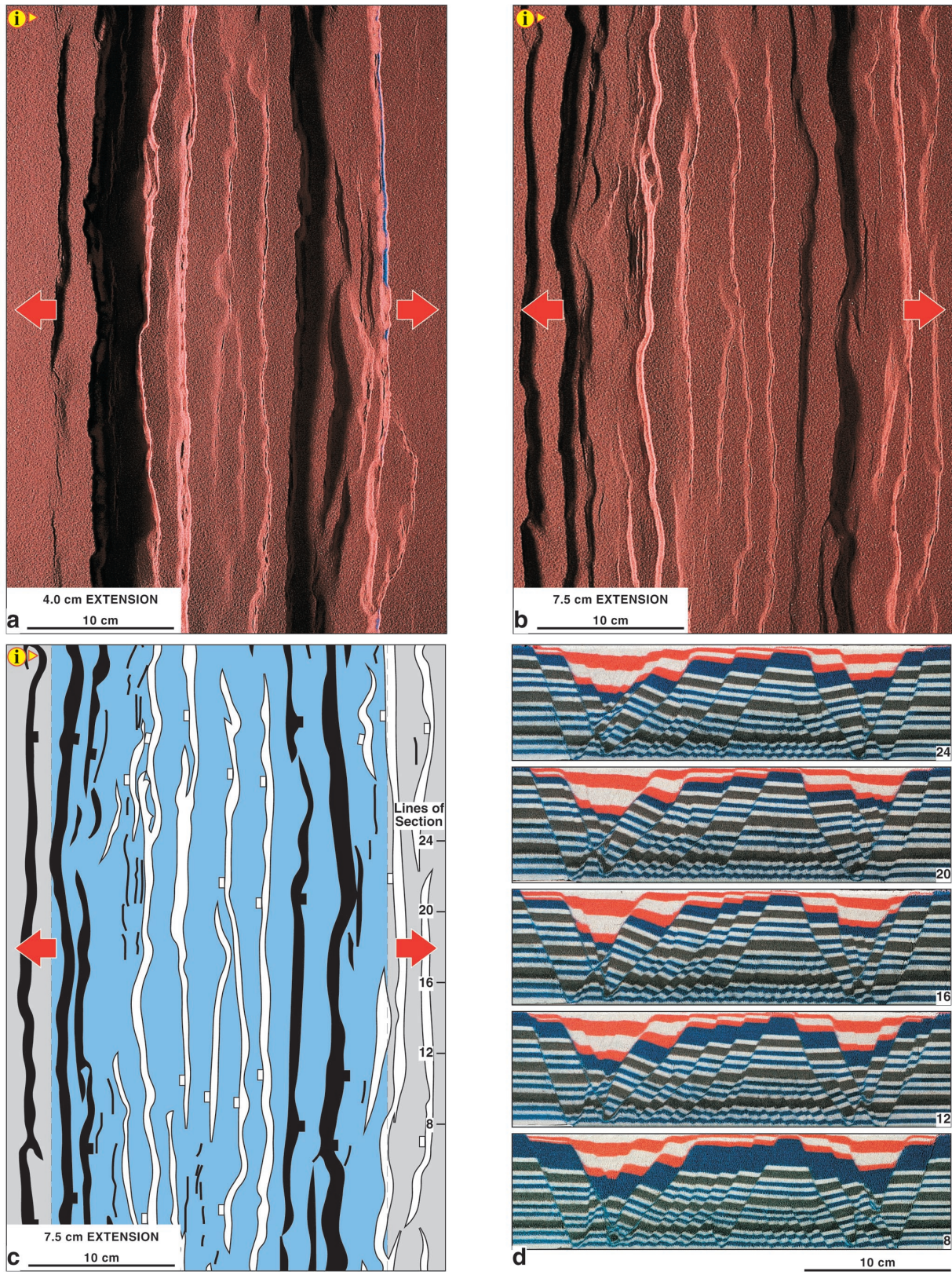


**Figure 4.** Analog model E 350: Orthogonal Rift. (a) Overhead view of analog model after 4 cm extension. Illumination is from the left. (b) Overhead view of analog model after 7.5 cm extension. Illumination is from the left. (c) Line diagram interpretation of the surface fault pattern at the end of extension. Dark bands are faults dipping to the right, and light bands are faults dipping to the left. The blue shading marks the stretched rubber sheet at the base of the model. (d) Serial sections through the orthogonal rift model. Synkinematic strata are the red and white layers at the top of the grabens on each side of the central intrarift horst block. Location of sections is indicated in (c).

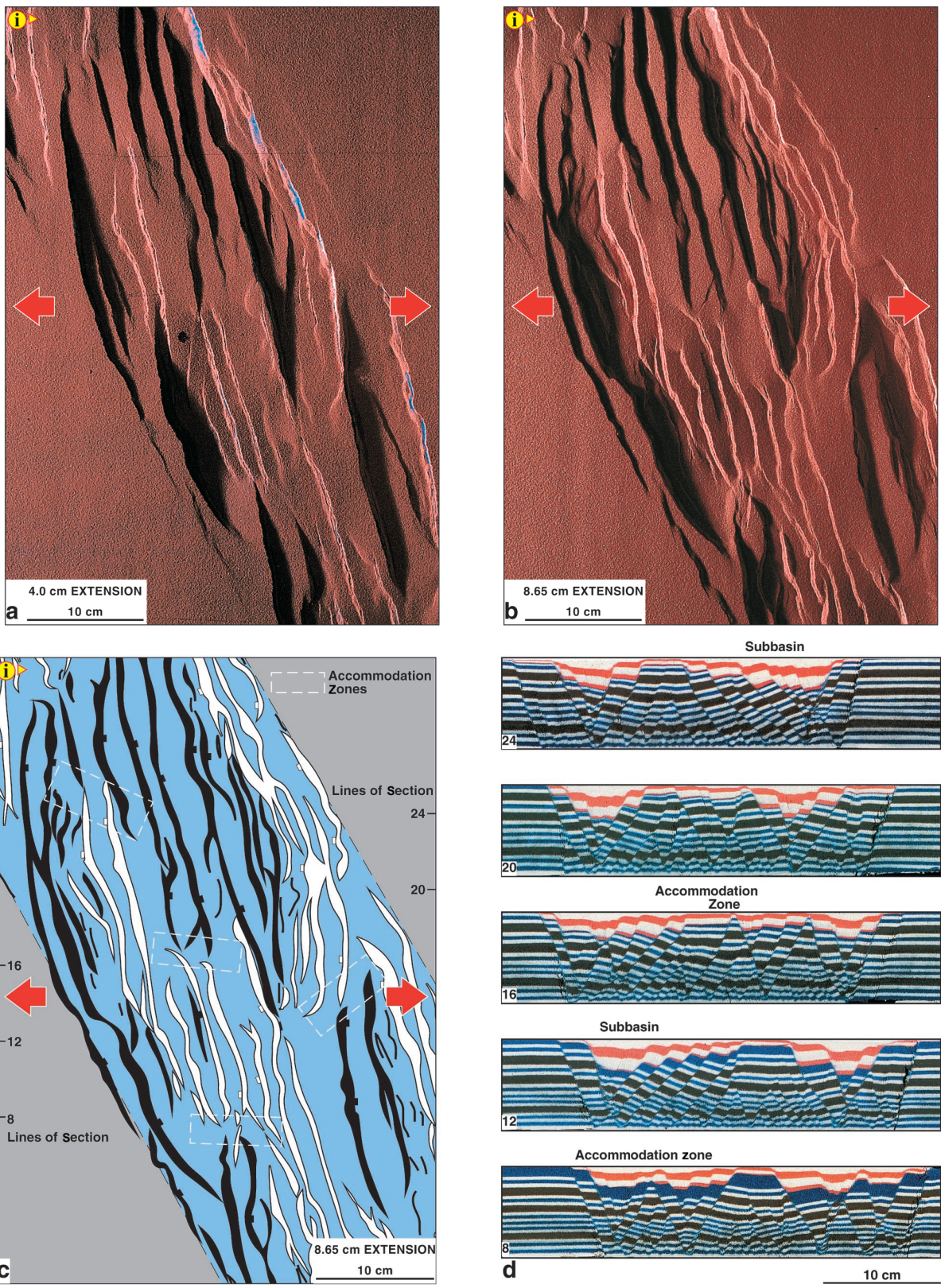


**Figure 5.** Analog model E 351: 60° Oblique Rift. (a) Overhead view of analog model after 4 cm extension. Illumination is from the left. (b) Overhead view of analog model after 8.65 cm extension (50% stretching at the base of the model). Illumination is from the left. (c) Line diagram interpretation of the surface fault pattern at the end of extension. Dark bands are faults dipping to the right, and light bands are faults dipping to the left. The blue shading marks the stretched rubber sheet at the base of the model. (d) Serial sections through the oblique rift model. Synkinematic strata are the red and white layers at the top of the grabens on each side of the central intrarift horst block. Location of sections is indicated in (c).

echelon fault segments. In part these were formed by the tips of major intrarift fault segments that curved into parallelism with the basement structural grain (Figure 5a). The intrarift fault arrays formed distinct, offset subbasins that developed on each side of the central rift axis. Using increased extension to 50% stretching at the base of the model, individual segments of the rift-border faults propagated along strike, breached the relay ramps, and linked, forming a semicontinuous rift-border fault system (Figure 5b). The intrarift faults increased their displacement and propagated along strike, forming accommodation zones where groups of like-dipping faults met groups of oppositely dipping faults (Figure 5b). Here, the tips of the opposing fault sets interlocked, producing a localized zone of conjugate faults commonly displaying divergent tips (Figure 5b). No strike-slip or oblique-slip transfer faults developed (Figure 5c). The along-strike changes in the subbasins and in the senses of fault dip are shown clearly on the vertical serial sections of the model (Figure 5d). Sections through the zones of offset between subbasins (section 8 in Figure 5d) show conjugate fault arrays and symmetrical graben structures.

In the 45° oblique model, the rift margin consisted initially of en echelon segments (Figure 6a). At low to moderate strains, the intrarift faults formed at high angles to the extension direction, producing a series of accommodation zones consisting of interlocking conjugate faults oblique to the extension direction (Figure 5a). Using increased extension, the tips of some of these intrarift faults propagated such that they curved parallel to the rift axis, forming much of the rift margin fault system (Figure 6b). Initial interlocking arrays of intrarift conjugate-fault systems developed into oblique accommodation zones characterized by tip divergence so extreme that the tips rotated into subparallelism with the rift axis (Figure 6b, c). Many of the intrarift faults display greater displacement than the major rift-margin structures (Figure 6b, c, d). Complex fault arrays developed, (Figure 6c) and the cross sections show both symmetrical and asymmetrical fault arrays (Figure 6d).

#### Offset Rift Models

Offset rift models (Figures 7, 8, 9) were produced by making a preextension offset in the rubber sheet at the base of the models (Figure 2c). These experiments produced strongly segmented rift models in which offset depocenters were separated by complex

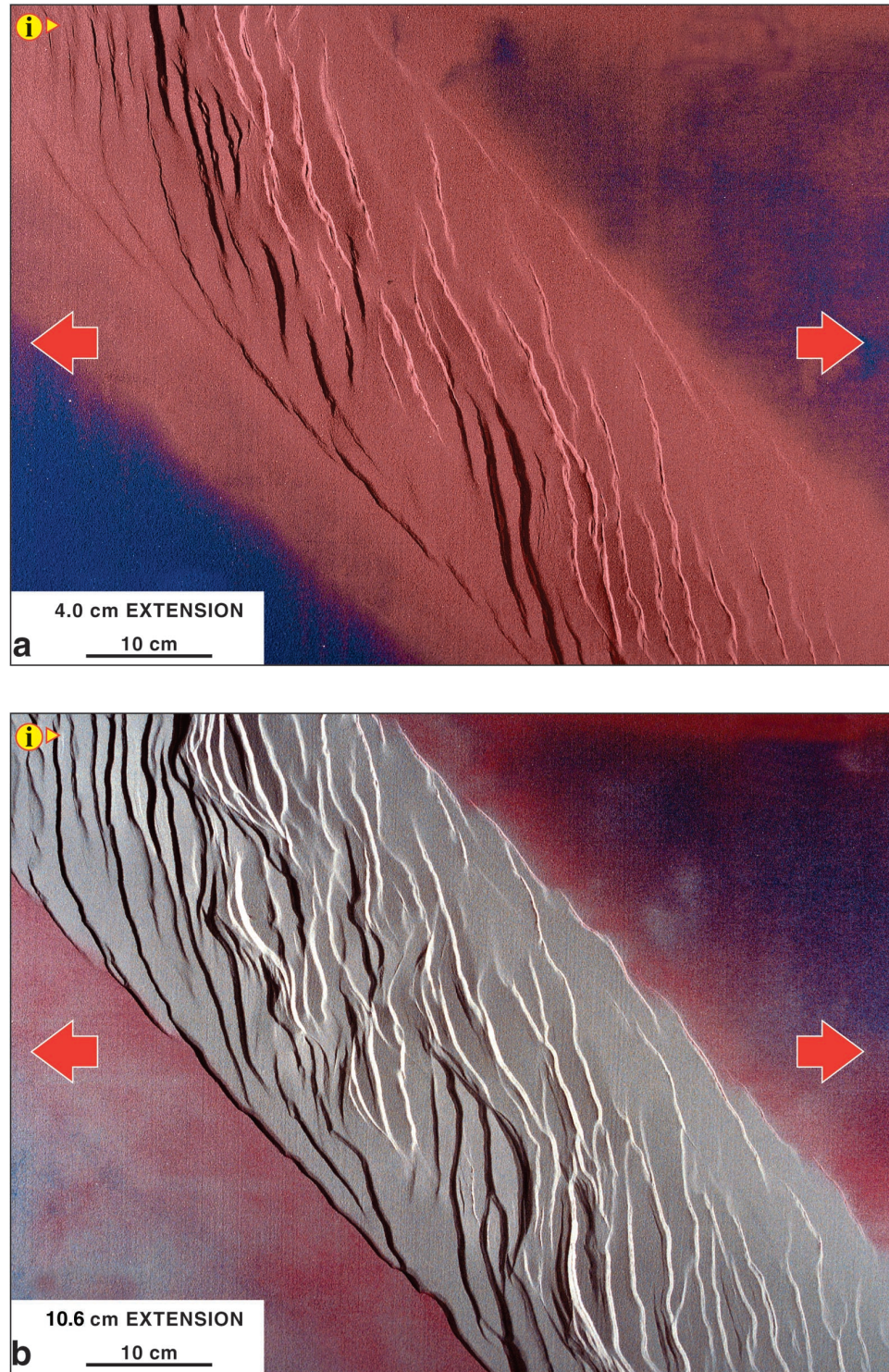
accommodation zones of interlinked faults without development of hard-linked strike-slip transfer faults (Figures 7, 8, 9).

In the offset-orthogonal rift model, distinct offset graben systems developed at low to moderate strains (Figure 7a). Both rift-border faults and intrarift faults were kinked with soft-linked relay ramps, and they breached relays above the offsets in the basal zone of stretching. Fault tips across these offset zones were strongly curved and overlapped, producing synthetic, interlocking arrays (Figure 7b). After 50% extension, the border faults were strongly curved and linked across the offsets, whereas the intrarift faults were more segmented (Figure 7b, c). In serial sections, the rift was typically symmetrical, having two grabens that developed adjacent to each border fault system; the graben axes stepped across the offset zones in the basement (Figure 7d).

The 60° and 45° offset rift models produced very similar rift structures (Figures 8, 9); both developed two different styles of accommodation zones above the offsets in the zone of basement stretching. At low values of extension above the left-stepping offset (lowermost offset in Figures 8, 9), a relatively high-relief accommodation zone formed parallel to the extension direction as a result of interlocking, oppositely dipping fault tips (Figures 8a, 9a). These interlocking faults display divergent fault-tip behavior (Figure 8b). In contrast, structurally low, oblique accommodation zones formed above the right-stepping basement offsets (uppermost offsets in Figures 8a, 9a). These were slightly oblique to the extension direction and consisted of highly curved, interlocking extensional fault tips. At 50% extension at the base of the model, the curved fault tips propagated along the accommodation zone and formed interlocking oblique-slip fault arrays (Figures 8b, 9b). The 45° offset model, in particular, developed small, elongate, rhomboidal subbasins in these low-relief, oblique accommodation zones (Figure 9b).

These offset rift models generated excellent examples of segmented dip domains, in which the dominant fault dip changed across the accommodation zones (Figures 8c, 9c). This is reflected in the serial sections that show a dominant half-graben asymmetry that flips polarity along strike across the offsets in the basal stretching zone (Figures 8d, 9d). As in the other analog models (e.g., Figures 4, 5, 6), no discrete strike-slip transfer faults were developed.

**Figure 6.** Analog model E 352: 45° Oblique Rift.  
 (a) Overhead view of analog model after 4 cm extension. Illumination is from the left.  
 (b) Overhead view of analog model after 10.6 cm extension (50% stretching at the base of the model). Illumination is from the left. Continued.



## DISCUSSION

### Analog Models

Analog models of orthogonal and offset-orthogonal rift systems produce characteristically simple rift systems

that are approximately cylindrical along strike (Figures 4, 7). The rifts are defined by long rift-border faults that formed by along-strike propagation of originally shorter, like-dipping segments that are linked by breaching of classic, synthetic relay ramps (Larsen, 1988; Peacock and Sanderson, 1991, 1994; Walsh and

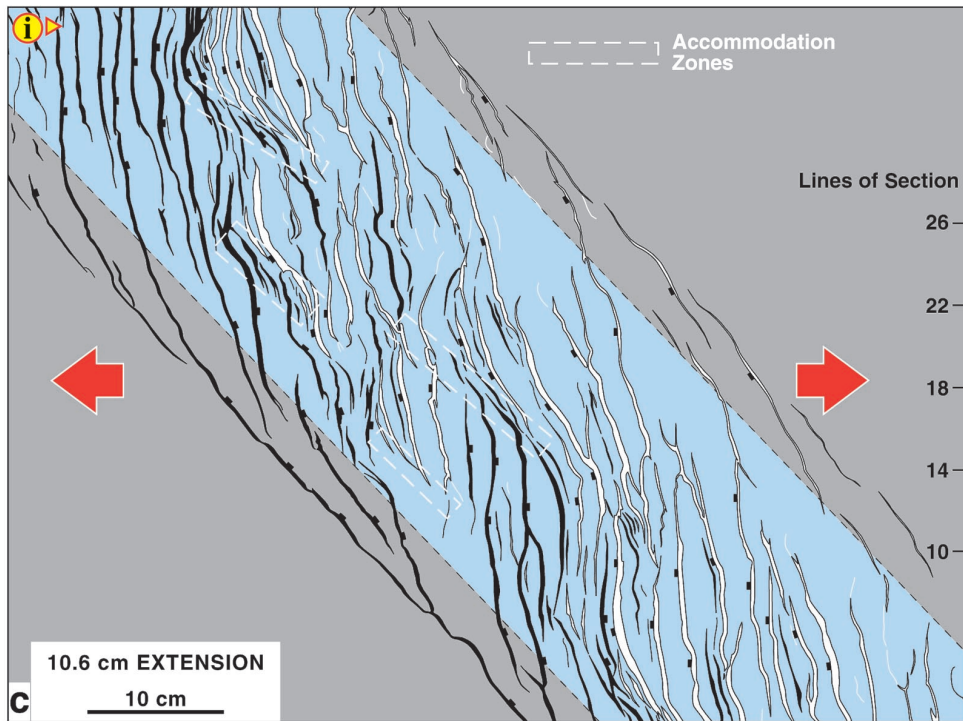
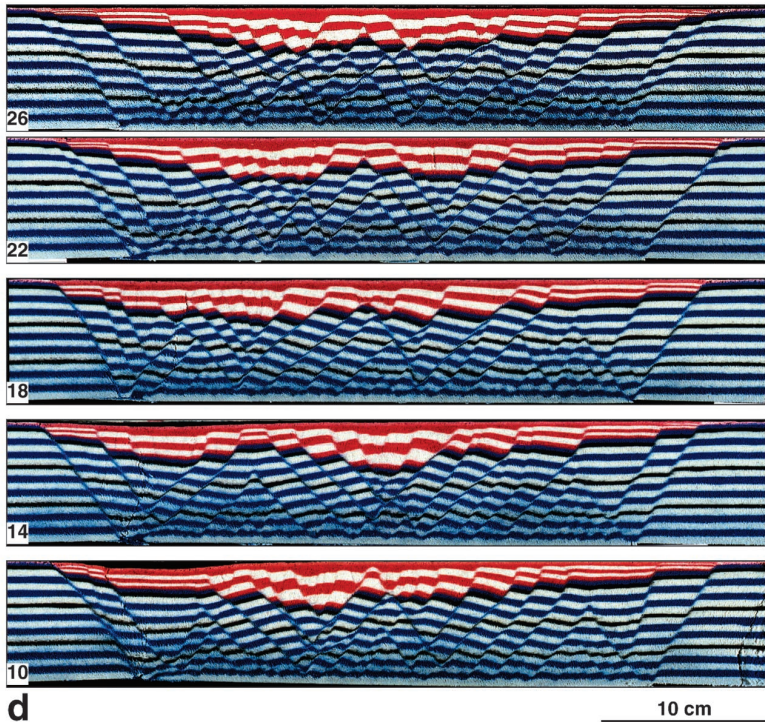


**Figure 6.** Continued. (c) Line diagram interpretation of the surface fault pattern at the end of extension. Dark bands are faults dipping to the right, and light bands are faults dipping to the left. The blue shading marks the stretched rubber sheet at the base of the model. (d) Serial sections through the oblique rift model. Synkinematic strata are the lighter layers at the top of the grabens on each side of the central intrarift horst block. Location of sections is indicated in (c).



Watterson, 1991; Childs et al., 1995) (Figures 4, 7). The long, linked rift-border faults commonly display constant displacement profiles along strike in the orthogonal rift model (Figure 4b). The intrarift zone of both these end members consists of two subbasins oriented at right angles to the extension direction and

separated by a linear (Figure 4) or offset (Figure 7) intrarift horst. The geometry of these orthogonal rift systems is set up very early in the experiment; it extends from between the central part of the rift and the rift margin and displays very little reorganization with increased extension. In the offset-orthogonal rift

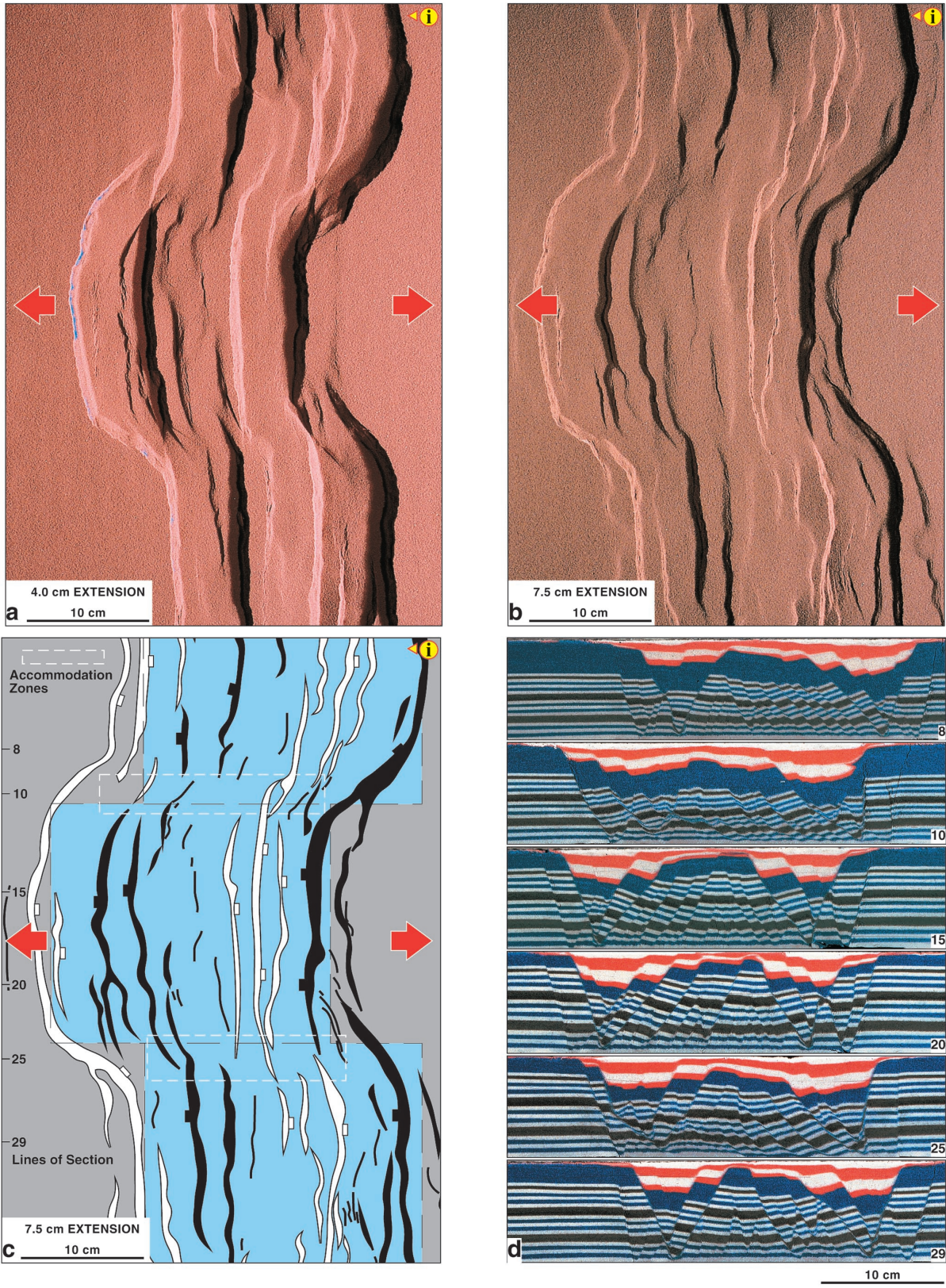


**Figure 7.** Analog model E 354: Offset-Orthogonal Rift. (a) Overhead view of analog model after 4 cm extension. (b) Overhead view of analog model after 7.5 cm extension (50% stretching at the base of the model). Illumination is from the right. (c) Line diagram interpretation of the surface fault pattern at the end of extension. Dark bands are faults dipping to the left, and light bands are faults dipping to the right. The blue shading marks the stretched rubber sheet at the base of the model. (d) Serial sections through the offset-orthogonal rift model. Synkinematic strata are the red and white layers at the top of the grabens on each side of the central intrarift horst block. Location of sections is indicated in (c).

system (Figure 7), the presence of a basal offset in the rift zone did not produce a discrete transfer fault in the cover. Cover deformation around the offset zones consisted of arcuate and linked rift-border faults and synthetic, interlocking fault arrays that define the intrarift subbasins (Figure 7).

In contrast to orthogonal rift systems, models run using oblique basement fabrics produce rift basins having segmented rift-border faults that closely parallel the rift axis, and intrarift fault domains that are oriented at a high angle to the extension vector (Figures 5, 6). Oblique rift systems display significant structural variations along the length of the rift zone, such as fault polarity switching that results in generation of intrarift subbasins. In the model rifts, domains of different fault polarities are separated by accommodation zones that are both parallel and oblique to the regional extension direction (Figures 7, 8). Transfer of displacement between subbasins and regional highs in these oblique models is effected by soft-linkage accommodation zones. In the  $60^\circ$  oblique rift model (Figure 5), these accommodation zones consisted of interlocking fault arrays of opposite dip polarities and divergent tips, which defined zones of relatively high relief in the rift interior (Figures 5, 10a). Such interlocking extensional fault arrays also have been observed in seismic data (Nichol et al., 1995) in which the conjugate fault zones were regions of significant fault damage that were necessary to accommodate the displacements on the oppositely dipping faults. These interlocking patterns were established very early in the experiments and had a profound effect on the evolution of the rift interior; they inhibited along-strike propagation of these fault arrays and thereby strongly influenced observed fault length:displacement ratios (Figure 5). In contrast, models run using  $45^\circ$  rift obliquity initially generated a similar pattern of interlocking opposite-polarity fault systems at low strains, but with increasing displacement, these accommodation zones evolved to oblique, low-relief accommodation zones (Figures 6, 10b). These accommodation structures were characterized by rotation of the tips of opposite-polarity faults into subparallelism with the rift axis, forming narrow, rhomboidal grabens subparallel to the axis of the rift (Figures 6, 10b).

Analog models of offset-oblique rifts generated subbasins that displayed major dip polarity changes above the hard-linked transfer zone in the basement (Figures 8, 9). In both of these offset rift systems ( $60^\circ$  and  $45^\circ$  oblique), two types of soft-linked accommodation zones were observed, dependent upon the sense

of basement offset with respect to the obliquity of the rift axis (Figures 8, 9, 10). High-relief accommodation zones are subparallel to the extension vector and are composed of interlocking opposite-polarity fault arrays characteristic of deformation above left-stepping rift segmentation (Figures 8, 9, 10a). Low-relief accommodation zones were generated above right-stepping rift segmentation. These zones consisted of opposite-polarity fault arrays that show strong rotation into the accommodation zone and generated composite accommodation zones oblique to the extension vector (Figures 8, 9, 10b). These accommodation zones are characterized by curvilinear grabens that crosscut the basement offset and are bounded by the rotated tips of the conjugate-fault sets (Figures 8, 9, 10b). The high degree of obliquity between the rotated tips of the conjugate-fault sets and the extension vector necessitates a degree of oblique slip along these zones.

Fault growth in the orthogonal and offset-orthogonal rift models shows similar features to those that would be expected if faults grew by a stress feedback mechanism (Cowie, 1998; Gupta et al., 1998; Cowie et al., 2000). In Cowie's models, initially isolated, optimally positioned faults rapidly link to form long, continuous, high-displacement fault zones, or soft-linked, high-displacement, segmented rift-border faults (cf. Cartwright et al., 1995). Orthogonal rift and offset-orthogonal rift models display this characteristic growth model, having rift-border and intrarift fault systems composed of long segments that are kinked where relay ramps have been breached. In our models of oblique rifts, rift-border fault zones are not continuous but consist of like-dipping fault segments linked by synthetic relay ramps parallel to the rift axis. This segmentation increases as the obliquity of the rift axis with respect to the stretching direction increases (e.g.,  $45^\circ$  rift in Figure 6), such that high-angle, intrarift faults in these models take up greater displacement than the border faults. These high-angle faults commonly display tip-line rotation at the rift margin into parallelism with the basement grain (e.g., Figure 5). Because of the position of these intrarift fault segments above a uniformly stretching basement, instead of a linear velocity discontinuity at the rift margin, they commonly form colinear arrays of opposite-polarity faults whose along-strike propagation is hindered by their interlocking tip lines, thus forming relatively high-relief accommodation zones (Figures 5, 6, 10). These interlocking accommodation features were formed early in the evolution of the experiments and are long lived, preventing the linkage of subbasins along the length of the rift.

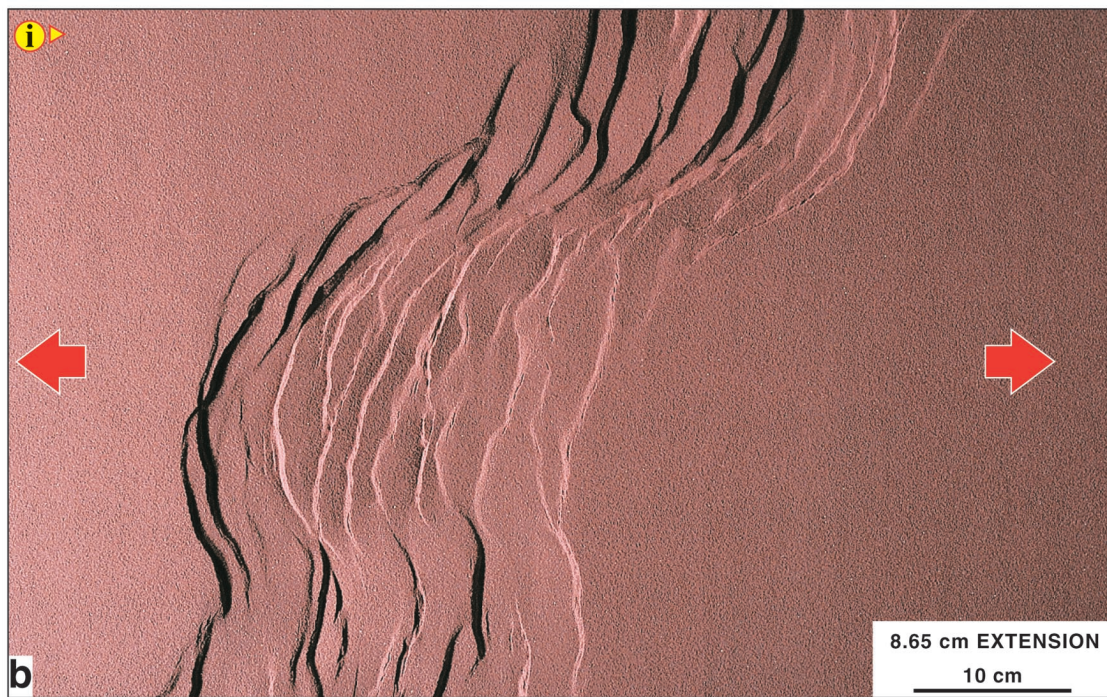
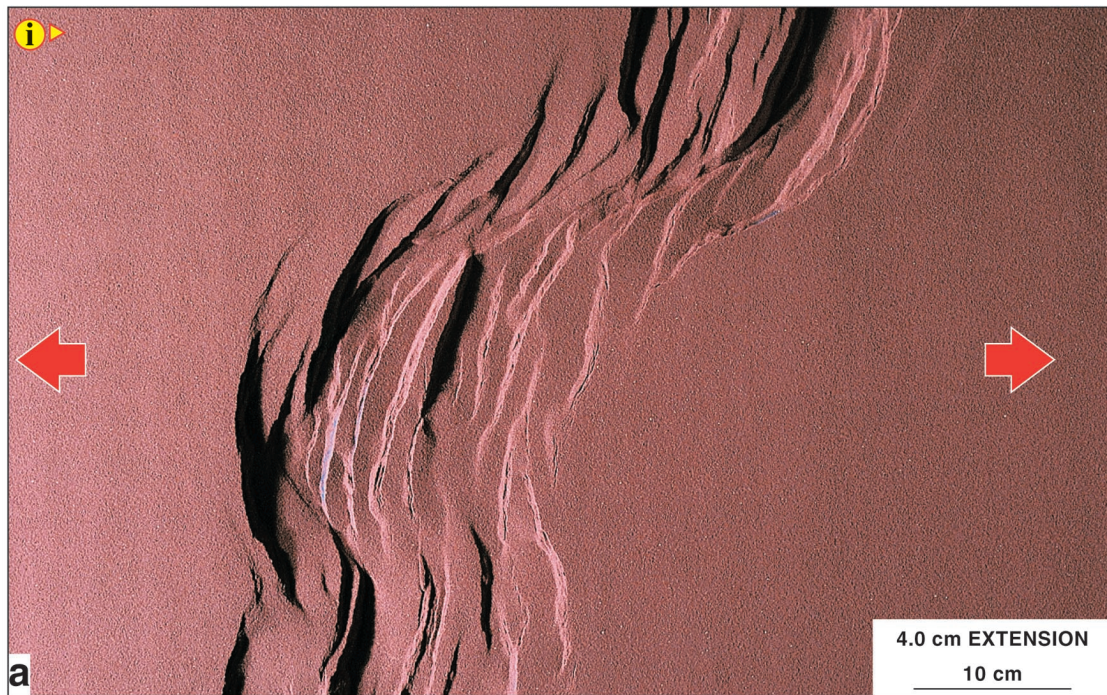


**Figure 8.** Analog model E 355: Offset 60° Oblique Rift. (a) Overhead view of analog model after 4 cm extension. Illumination is from the left. (b) Overhead view of analog model after 8.65 cm extension (50% stretching at the base of the model). Illumination is from the left. Continued.

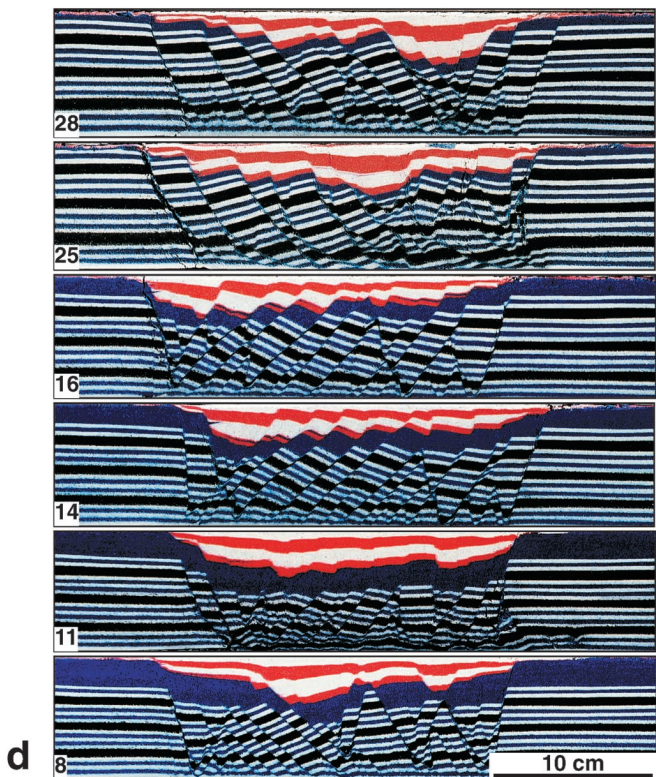
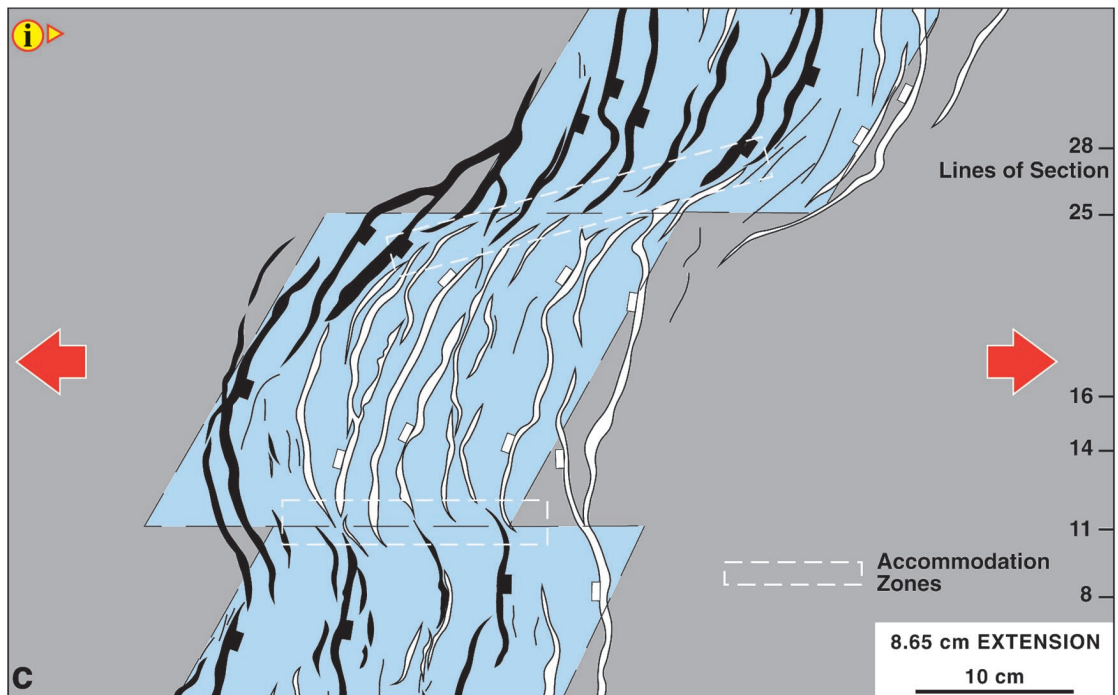
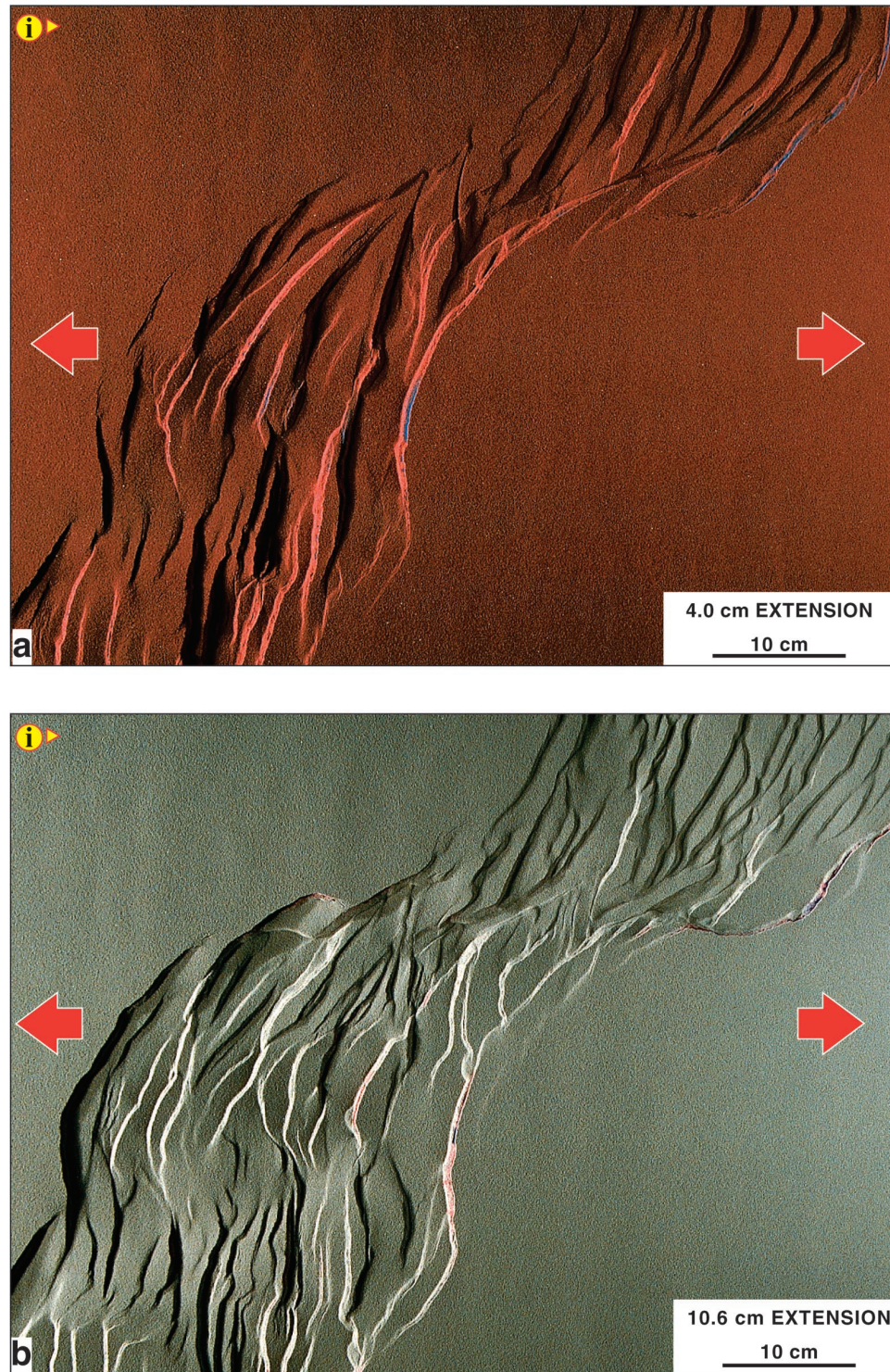


**Figure 8.** Continued. (c) Line diagram interpretation of the surface fault pattern at the end of extension. Dark bands are faults dipping to the right and light bands are faults dipping to the left. The blue shading marks the stretched rubber sheet at the base of the model. (d) Serial sections through the offset oblique rift model. Synkinematic strata are the red and white layers at the top of the grabens on each side of the central intrarift horst block. Location of sections is indicated in (c).

**Figure 9.** Analog model E 356: Offset 45° Oblique Rift. (a) Overhead view of analog model after 4 cm extension. Illumination is from the left. (b) Overhead view of analog model after 10.6 cm extension (50% stretching at the base of the model). Illumination is from the left. Continued.



### Comparisons with Natural Examples of Rift Systems

The scaled analog models of rift fault systems described in this article show many similarities to both outcrop and subsurface fault patterns of natural rifts. Whereas geometrical similarities do not in them-

selves imply similar deformation mechanisms and evolution pathways for the model geometries and the natural examples, strong resemblances exist in their fault styles, patterns, and modes of propagation and linkage to make reasonable comparisons between them.

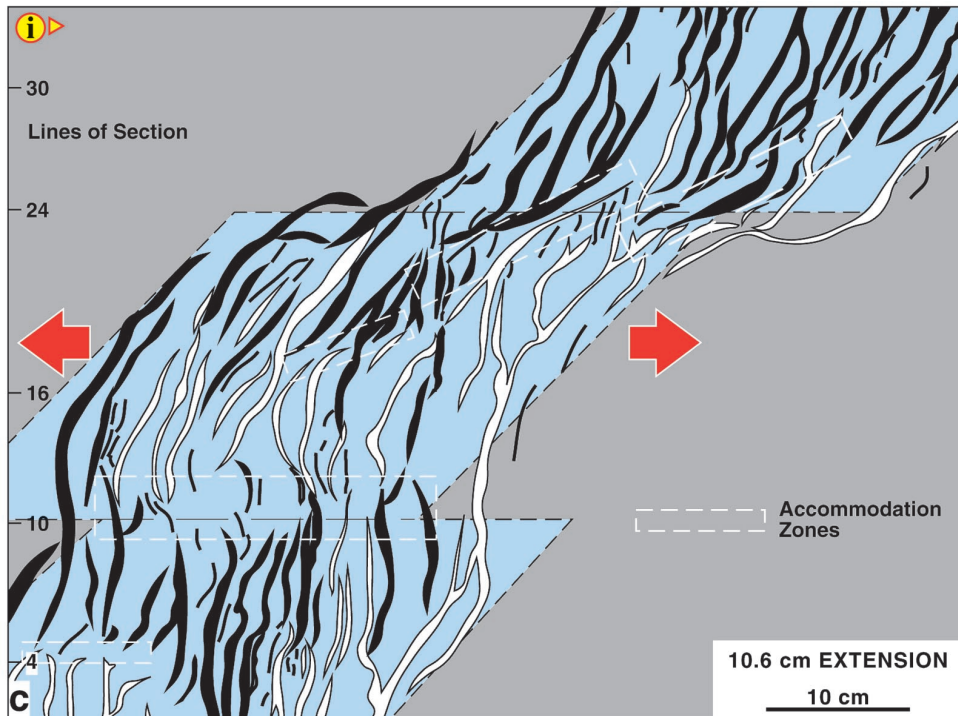
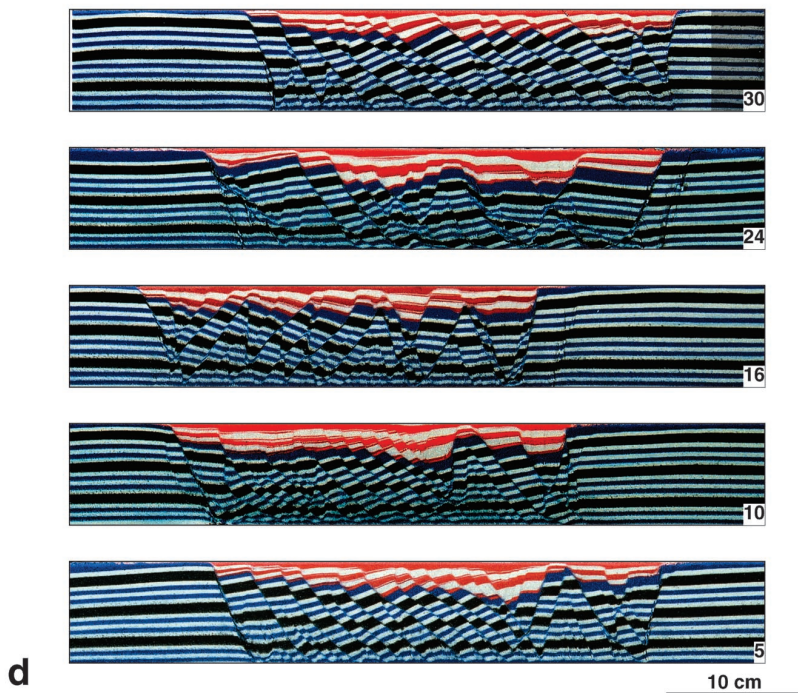


**Figure 9.** Continued. (c) Line diagram interpretation of the surface fault pattern at the end of extension. Dark bands are faults dipping to the right, and light bands are faults dipping to the left. The blue shading marks the stretched rubber sheet at the base of the model. (d) Serial sections through the offset oblique rift model. Synkinematic strata are the red and white layers at the top of the grabens on each side of the central intrarift horst block. Location of sections is indicated in (c).



### Orthogonal Rifts

The Gregory rift in East Africa shows excellent examples of segmented rift-border fault systems, as well as long, relatively straight, intrarift faults in synrift Miocene volcanic units (Figure 11). Both the rift-border

and intrarift faults are dominantly north-south striking and have long overlap regions between adjacent faults. Along-strike displacement transfer is by soft-linked relay-ramp structures, and no strike-slip or oblique-slip transfer faults are found (cf. Bosworth et al., 1986).

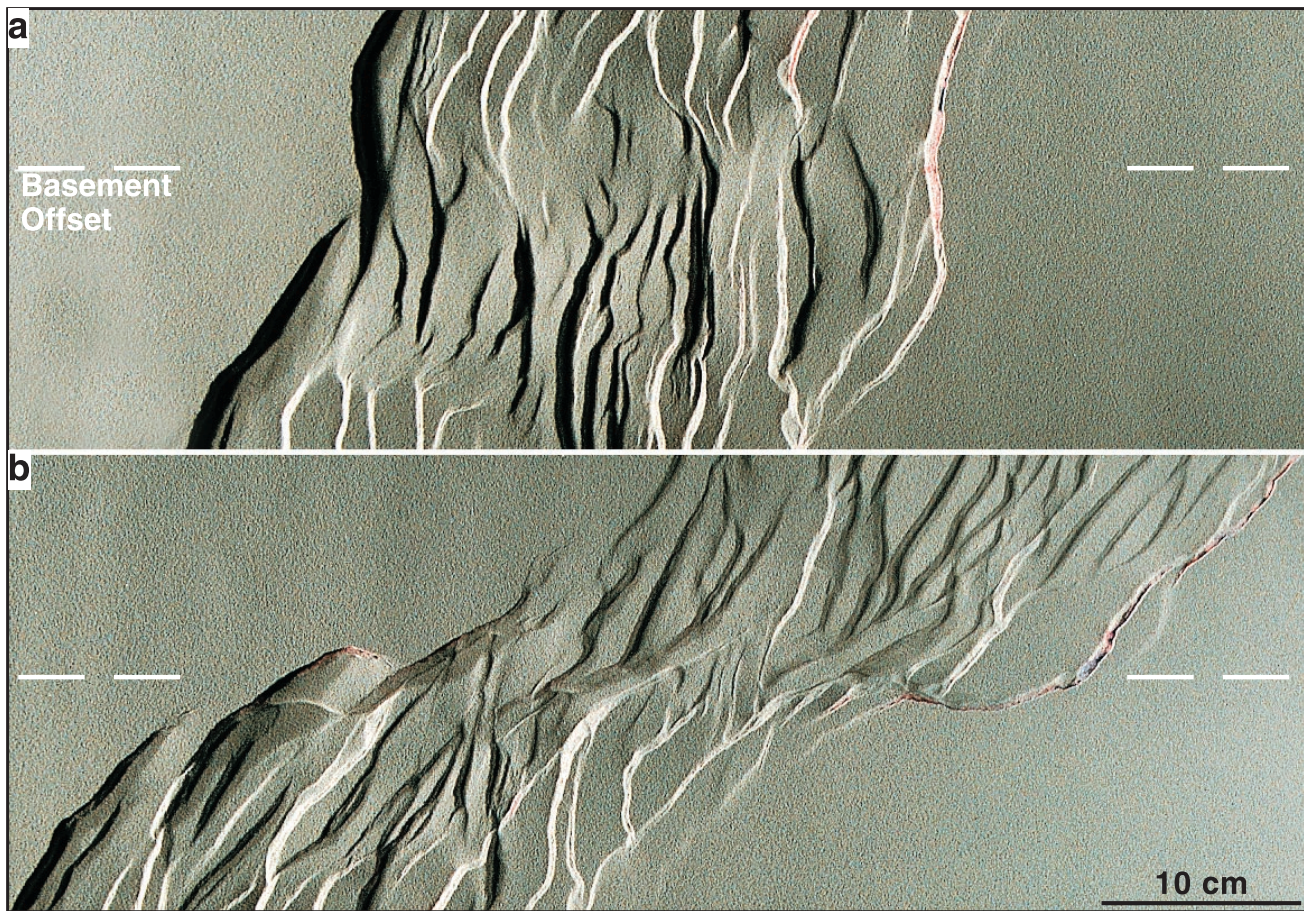


**Figure 10.** Accommodation zones formed in the model rifts. (a) Detail of an analog model of a low-strain, relatively high-relief accommodation zone parallel/subparallel to the extension direction. (b) Detail of an analog model of a high-strain, relatively low-relief accommodation zone oblique to the extension direction. Illumination is from the left.

Extensional fault patterns having a similar lack of discrete, hard-linked strike-slip transfer faults also have been observed in other parts of the East African-Ethiopian rift system (cf. Ebinger, 1989a, b; Kronberg, 1991; Hayward and Ebinger, 1996). Where originally segmented extensional faults have linked by breaching of the relay ramps, distinct kinked-fault traces are developed (Figure 11a, b). This pattern is directly analogous to the model rift-fault patterns developed in the orthogonal rift model (Figure 4) and indicate that the extension direction was dominantly east-west (cf. Bosworth et al., 1986), orthogonal to the dominant intra-rift and rift marginal-fault systems. Patterns of initial-fault segmentation and subsequent linkage similar to those in the analog models also have been found in three-dimensional (3-D) seismic studies of Jurassic faults in the Viking Graben, North Sea (McLeod et al., 2000).

#### Oblique and Offset Rifts

Oblique rifts are characterized by en echelon rift marginal-fault systems oblique to the extension direction and intrarift faults orthogonal to the extension direction (Figures 5, 6). Radar imagery from the extended volcanic tablelands in Owens Valley, north of Bishop, California, shows the 700 ka Bishop tuff down-thrown in a north-northwest-trending extensional structure (Figure 12). The margins of this zone of extension are oblique to the east-west-oriented extension (e.g., Dawers et al., 1993; Dawers and Anders, 1995) (Figure 12a). The marginal-fault systems are characterized by distinct relay-ramp structures, whereas the internal faults, although sparsely developed, are at high angles to the extension direction and are linked by breached relay ramps (Figure 12b). In a similar fashion to structures seen in the 60° oblique-rift model, parts of the marginal-fault system are composed of

north-south, intrarift segments that rotate along strike and link, to form the north-northwest-trending margin (see Figures 5, 12).

Two examples of offset grabens and rift systems are shown in Figures 13 and 14. In the Canyonlands example, the extension direction is orthogonal to the series of discrete and linked grabens that form the rift system (Trudgill and Cartwright, 1994) (Figure 13). An extension-parallel accommodation zone allows transfer of displacement along strike between grabens 1 and 3 and is accommodated by synthetic interlocking fault arrays defining graben 2 and separated by major relay structures (Figure 13). In the southern Rio Grande rift, the Redford Lajitas transfer zone accommodates displacement transfer between the northern subbasin (Redford Bolson) and the southern subbasin (Big Bend National Park area) (Henry, 1998). Fault-plane solutions and slickenside data indicate a dominant east-northeast extension direction in this region, which is oblique to most of the mapped surface faults (Henry, 1998) (Figure 14). Dextral oblique slip is recorded from faults in the Redford Lajitas structure. The narrow Santana Bolson in this zone displays the lowest structural relief in the region (Henry, 1998); it is similar to oblique accommodation structures found above right steps in the 60° and 45° offset rift models (Figures 8, 9, 10b, 14). The Redford Lajitas transfer/accommodation zone is situated above a deeply buried east-west basement structure that is similar in orientation to the basement offsets in the models. Further, to the north of the area illustrated in Figure 15 is the Tascotal Mesa fault, a prominent east-west-trending transfer fault that has demonstrable dextral slip along its length transferring displacement eastward from the Redford Bolson to the Presidio Bolson (Henry, 1998). The difference in style between these two transfer or accommodation structures is attributed to the shallow depth to basement below the Tascotal Mesa structure (Henry, 1998). Basement control on the development of accommodation zones in the Gulf of Suez rift is also described in Younes and McClay (2002).

The comparative examples of natural rift-fault patterns, together with the analog models described in this article, have enabled the construction of several conceptual models for the progressive evolution of rift-fault patterns in plan view (Figure 15). These diagrams illustrate the predicted initial fault patterns at low values of extension ( $\beta = 1.1 - 1.3$ ) and at higher extensions ( $\beta > 1.5$ ), where originally segmented faults have linked along strike (Figure 15). Changes in subbasin

(fault) polarities in these diagrams are indicated by the development of accommodation zones formed by overlapping and interlocking fault arrays. The 3-D synoptic models of the two dominant types of accommodation zone, the high-relief extension-parallel accommodation zone (characteristic of some orthogonal rift systems) and the low-relief oblique accommodation zone (as observed in many of the models described in this article), are shown in Figure 16.

## CONCLUSIONS

Analog models of oblique, stepped, and offset rifts characteristically produced rift-border fault systems that linked by means of classic, synthetic relay ramps. In the model rifts, however, domains of different fault polarities are separated by accommodation zones that are both parallel (subparallel) and oblique to the regional extension direction. In the extension-parallel accommodation zones, the tips of oppositely dipping faults curve away from each other, forming an anticlinal-like zone of high relief. Oblique accommodation zones evolve from simple, interlocking arrays to form structural lows defined by oblique-slip faults that parallel the rotated tips of the opposite-polarity fault sets. In cross section, the accommodation zones consist of conjugate fault arrays formed by the interlocking tips of oppositely dipping domino fault systems. In the models, the accommodation zones form early in the evolution of the rift and persist throughout the experiment history, thus influencing the ability of faults to propagate along strike, prolong basin segmentation, and in some cases, notably influence the fault length/displacement profiles.

The analog models and the natural examples show that the architectures of rifts and, in particular, along-strike switches in basin polarities and dominant fault dips across accommodation zones are more complicated than previously published models of simple overlapping or interlocking rift-border fault systems. The models developed two styles of accommodation zones, both formed by interlocking, overlapping, intrarift fault tips. High-relief accommodation zones are parallel or mildly oblique to the extension direction, whereas low-relief accommodation zones are highly oblique to the extension and are bounded by oblique-slip fault systems. No hard-linked, extension-parallel, strike-slip or oblique-slip transfer faults were developed in the models, in direct contrast to the extension-parallel, strike-slip or oblique-slip transfer fault model



**Figure 11.** East African rift system, Kenya. (a) Landsat thematic mapper (TM) image of the Gregory rift west of Nairobi, Kenya. Continued.

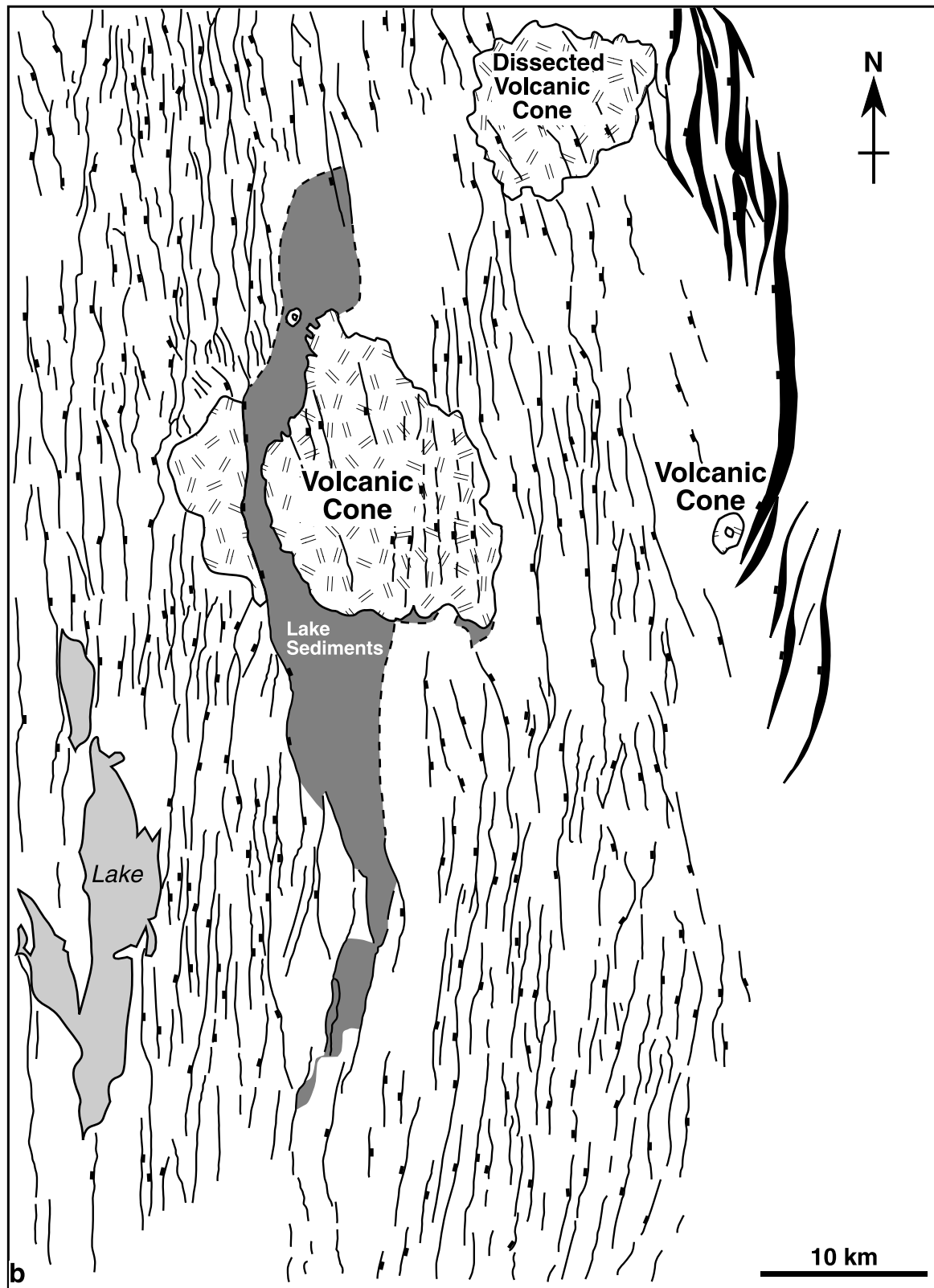
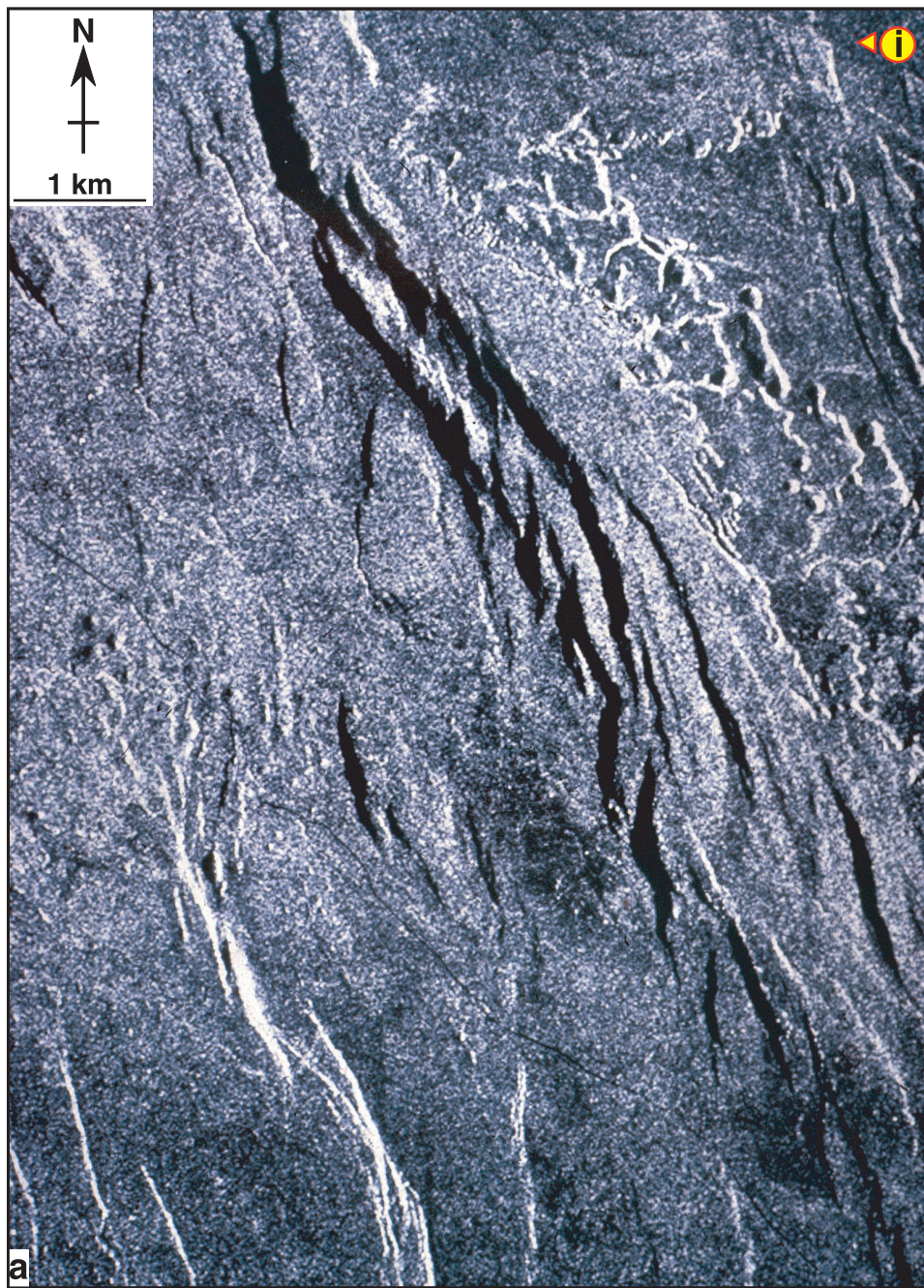


**Figure 11.** Continued. (b) Line diagram interpretation of (a) showing the segmented and slightly offset rift-border fault system on the east and a high density of north-south-oriented intrarift faults in the main part of the rift. This pattern is characteristic of orthogonal rifting with the dominant extension direction oriented east-west.

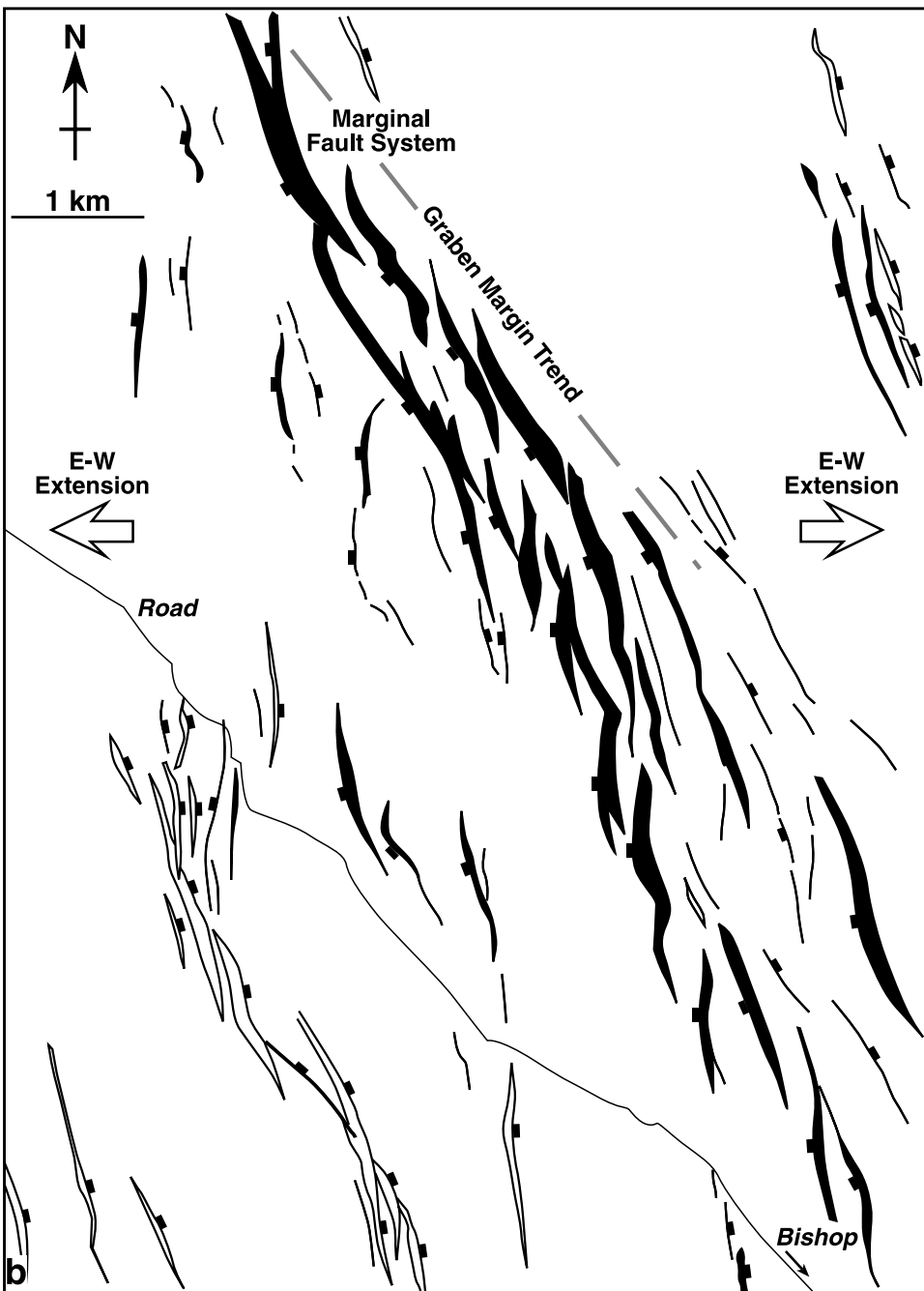
**Figure 12.** (a) Radar image of the volcanic tablelands, Bishop, California. The image shows a series of en echelon marginal faults in the Bishop tuff running obliquely across the image with north-south-oriented interior faults in the center left of the image. (Image courtesy of Conoco Exploration.) Continued.



commonly used to account for depocenter changes and fault-polarity switches in rift systems.

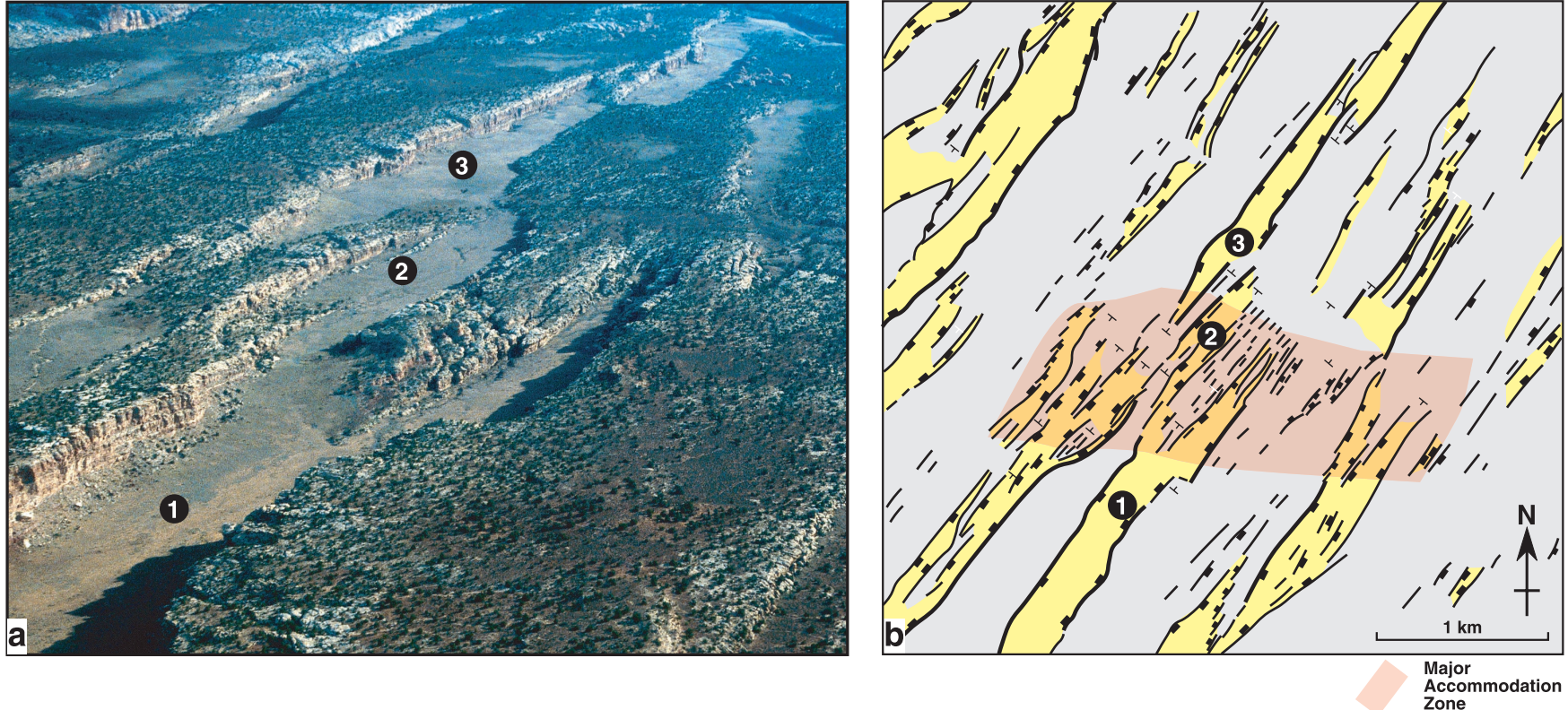
#### REFERENCES CITED

- Bally, A. W., 1981, Atlantic type margins, in *Geology of passive continental margins: history, structure and sedimentologic record*: AAPG Education Course Notes Series 19, p. 1–48.
- Bosworth, W., 1985, Geometry of propagating continental rifts: *Nature*, v. 316, p. 625–627.
- Bosworth, W., 1994, A high-strain rift model for the southern Gulf of Suez (Egypt), in J. J. Lambiase, ed., *Hydrocarbon habitat in rift basins*: Geological Society Special Publication 80, p. 75–102.
- Bosworth, W., P. Crevello, R. D. Winn Jr., and J. Steinmetz, 1986, A new look at Gregory's rift: the structural style of continental rifting: *EOS*, v. 67, p. 577, 582–583.
- Cartwright, J. A., B. D. Trugdill, and C. S. Mansfield, 1995, Fault growth by segment linkage: an explanation for scatter in maximum displacement and trace length data from the Canyonlands grabens of SE Utah: *Journal of Structural Geology*, v. 17, p. 1319–1326.
- Childs, C., J. Watterson, and J. J. Walsh, 1995, Fault overlap zones

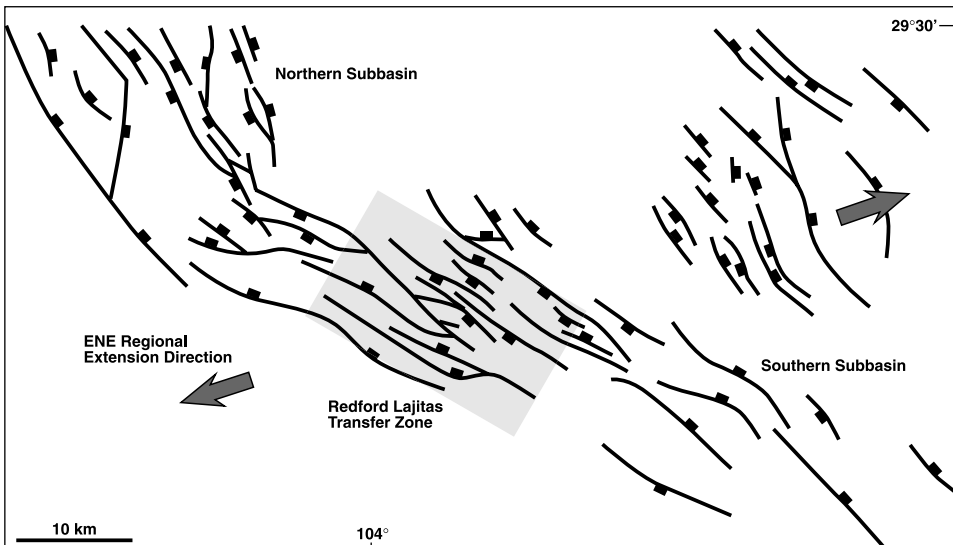


**Figure 12.** Continued.  
(b) Line diagram interpretation of (a). This image is an example of oblique rifting with the extension direction oriented east-west.

- within developing normal fault systems: *Journal of the Geological Society*, v. 152, p. 535–549.
- Cloos, E., 1968, Experimental analysis of Gulf Coast fracture patterns: *AAPG Bulletin*, v. 52, p. 420–444.
- Cowie, P. A., 1998, A healing-reloading feedback control on the growth rate of seismogenic faults: *Journal of Structural Geology*, v. 20, p. 1075–1087.
- Cowie, P. A., S. Gupta, and N. H. Dawers, 2000, Implications of fault array evolution for synrift depocentre development: insights from a numerical fault growth model: *Basin Research*, v. 12, p. 241–261.
- Dawers, N. H., and M. A. Anders, 1995, Displacement-length scaling and fault linkages: *Journal of Structural Geology*, v. 17, p. 607–614.
- Dawers, N. H., M. H. Anders, and C. H. Scholtz, 1993, Growth of normal faults: displacement-length scaling: *Geology*, v. 21, p. 1107–1110.
- Ebinger, C. J., 1989a, Geometric and kinematic development of border faults and accommodation zones, Kivu-Rusizi rift, Africa: *Tectonics*, v. 8, p. 117–137.
- Ebinger, C. J., 1989b, Tectonic development of the western branch of the East African rift system: *Geological Society of America Bulletin*, v. 101, p. 885–903.
- Etheridge, M. A., J. C. Branson, and P. G. Stuart-Smith, 1987, The



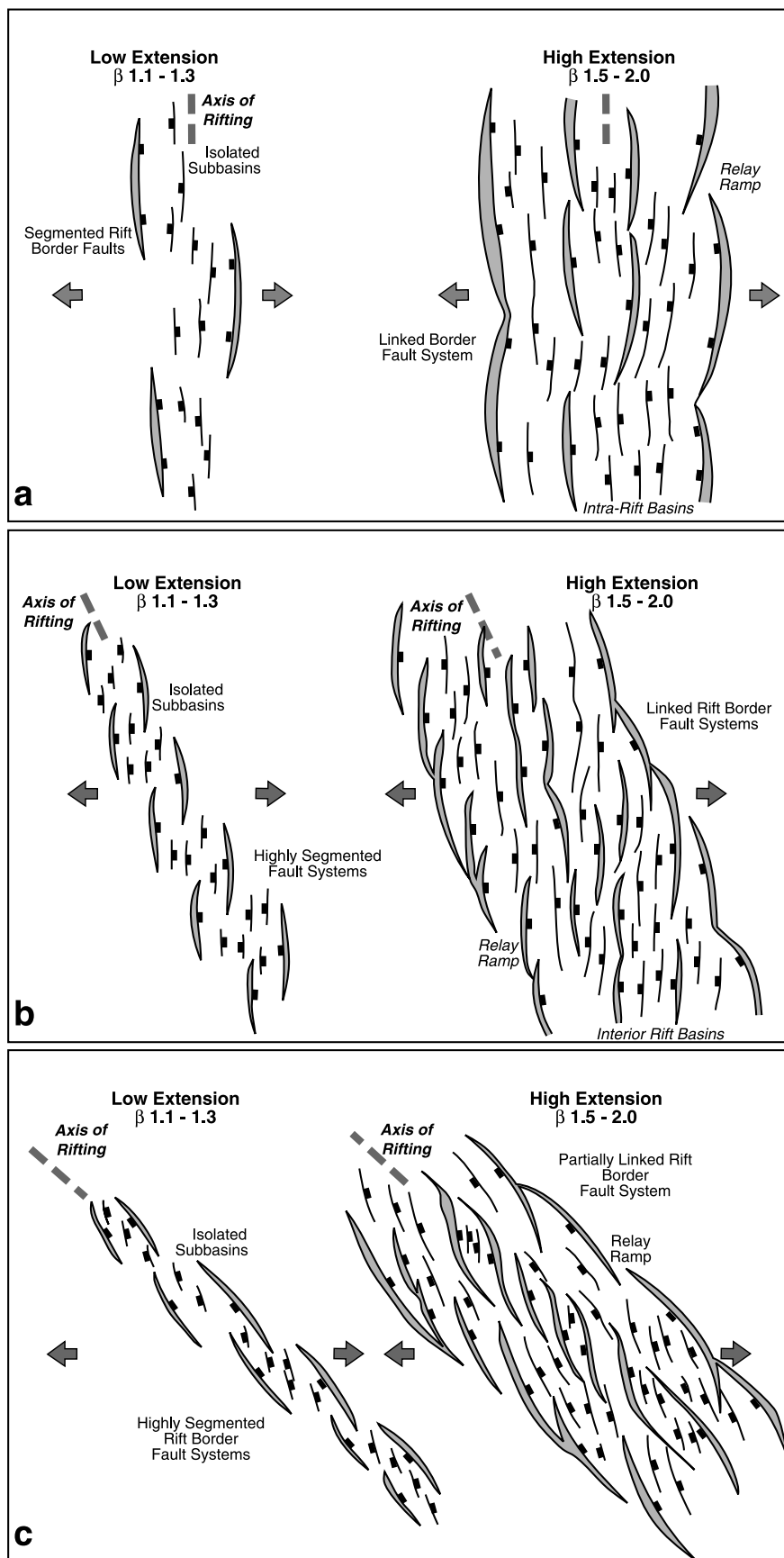
**Figure 13.** (a) Oblique aerial photograph of offset grabens (1, 2, 3) in Canyonlands National Park, Utah. At the terminations of individual grabens, the main faults branch into a series of splays that form relay ramps between overlapping, like-dipping faults and complex, conjugate arrays between oppositely dipping faults. (b) Sketch map of the graben systems in Canyonlands National Park, Utah, showing a series of offset graben systems formed by orthogonal extension and linked by complex accommodation zones of interlocking faults.



**Figure 14.** Map of offset grabens and the oblique Redford Lajitas transfer zone, southern Rio Grande rift, Texas (modified from Henry, 1998). Extension direction is averaged from data along the length of the extensional system.

- Bass, Gippsland and Otway basins, southeast Australia: a branched rift system formed by continental extension, in C. Beaumont and A. J. Tankard, eds., Sedimentary basins and basin-forming mechanisms: Canadian Society of Petroleum Geologists Memoir 12, p. 147–162.
- Faugere, E., and J. P. Brun, 1984, Modelisation expérimentale de la distension continentale: Compte Rendu Académie des Sciences Paris, v. 229, ser. II, p. 365–370.
- Faulds, J. E., and R. J. Varga, 1998, The role of accommodation zones and transfer zones in the regional segmentation of extended terranes, in J. E. Faulds and J. H. Stewart, eds., Accommodation zones and transfer zones: the regional segmentation of the Basin and Range province: Geological Society of America Special Paper 323, p. 1–46.
- Gibbs, A. D., 1983, Balanced section constructions from seismic sections in areas of extensional tectonics: Journal of Structural Geology, v. 5, p. 153–160.
- Gibbs, A. D., 1984, Structural evolution of extensional basin margins: Journal of the Geological Society, v. 141, p. 609–620.
- Gibbs, A. D., 1987, Development of extension and mixed-mode sedimentary basins, in M. P. Coward, J. F. Dewey, and P. L. Hancock, eds., Continental extensional tectonics: Geological Society Special Publication 28, p. 19–33.
- Gupta, S., P. A. Cowie, N. H. Dawers, and J. R. Underhill, 1998, A mechanism to explain rift-basin subsidence and stratigraphic patterns through fault array evolution: Geology, v. 26, p. 595–598.
- Hayward, N., and C. J. Ebinger, 1996, Variations in the along-axis segmentation of the Afar rift system: Tectonics, v. 15, p. 244–257.
- Henry, C. D., 1998, Basement-controlled transfer zones in an area of low-magnitude extension, eastern Basin and Range province, Trans-Pecos Texas in J. E. Faulds and J. J. Stewart, eds., Accommodation zones and transfer zones: the regional segmentation of the Basin and Range province: Geological Society of America Special Paper 323, p. 75–89.
- Horsfield, W. T., 1977, An experimental approach to basement-controlled faulting: Geologie en Mijnbouw, v. 56, p. 363–370.
- Horsfield, W. T., 1980, Contemporaneous movement along crossing conjugate normal faults: Journal of Structural Geology, v. 2, p. 305–310.
- Karner, G. D., and N. W. Driscoll, 1999, Tectonic and stratigraphic development of the west African and eastern Brazilian margins: insights from quantitative basin modelling, in N. R. Cameron, R. H. Bate, and V. S. Clure, eds., The oil and gas habitats of the South Atlantic: Geological Society Special Publication 153, p. 11–40.
- Kronberg, P., 1991, Geometries of extensional fault systems, observed and mapped on aerial and satellite photographs of Central Afar (Ethiopia/Djibouti): Geologie en Mijnbouw, v. 70, p. 145–161.
- Larsen, P., 1988, Relay structures in a Lower Permian basement-involved extension system, East Greenland: Journal of Structural Geology, v. 10, p. 3–8.
- Lister, G. S., M. A. Etheridge, and P. A. Symonds, 1986, Detachment faulting and the evolution of passive continental margins: Geology, v. 14, p. 246–250.
- McClay, K. R., 1990a, Extensional fault systems in sedimentary basins: a review of analogue model studies: Marine and Petroleum Geology, v. 7, p. 206–233.
- McClay, K. R., 1990b, Deformation mechanics in analogue models of extensional fault systems, in R. J. Knipe and E. H. Rutter, eds., Deformation mechanisms, rheology and tectonics: Geological Society Special Publication 54, p. 445–453.
- McClay, K. R., and M. White, 1995, Analogue models of orthogonal and oblique rifting: Marine and Petroleum Geology, v. 12, p. 137–151.
- McLeod, A., N. H. Dawers, and J. R. Underhill, 2000, The propagation and linkage of normal faults: insights from the Strathspay-Brent-Stratfjord fault array, northern North Sea: Basin Research, v. 12, p. 263–284.
- Morley, C. K., 1994, Structural geology of rifts, in J. J. Lambiase, ed., Hydrocarbon habitat in rift basins: Geological Society Special Publication 80, p. 75–102.
- Morley, C. K., R. A. Nelson, T. L. Patton, and S. G. Munn, 1990, Transfer zones in the East African rift system and their relevance to hydrocarbon exploration in rifts: AAPG Bulletin, v. 74, p. 1234–1253.
- Moustafa, A. R., 1997, Controls on the development and evolution of transfer zones: the influence of basement structure and sedimentary thickness in the Suez rift and Red Sea: Journal of Structural Geology, v. 19, p. 755–768.

**Figure 15.** Conceptual extensional fault patterns for orthogonal and oblique rift systems. These patterns are based partly on results of analog models described in this article, as well as our studies of natural rift systems. (a) Orthogonal rift fault systems. (b) Moderately oblique rift fault systems. (c) Strongly oblique rift fault systems.



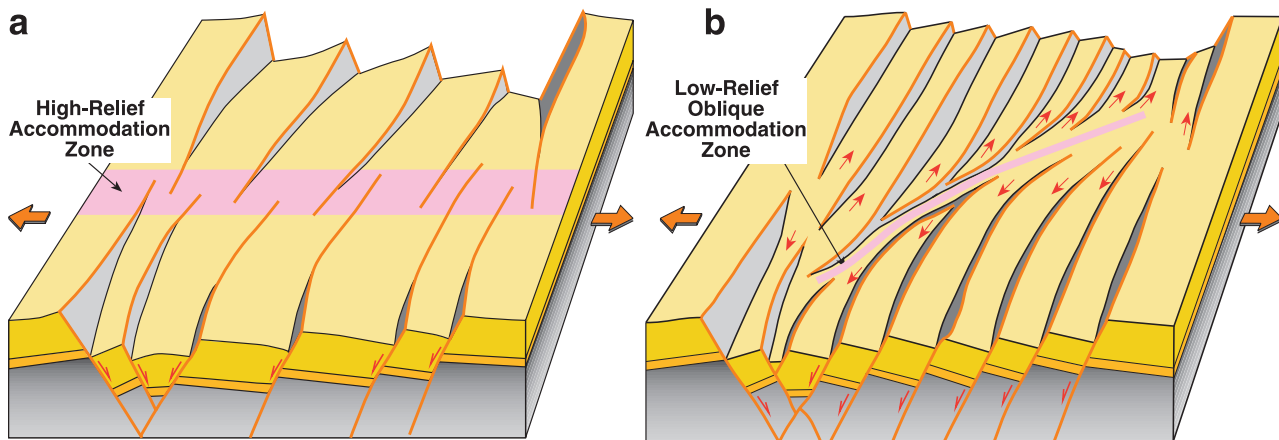


**Figure 16.** Accommodation zone models. (a) Conceptual 3-D model of a low-strain accommodation zone parallel to the dominant extension direction. This zone is formed by interlocking arrays of oppositely dipping faults and is typically found above obtusely oriented basement transfer faults or in offset-orthogonal rift systems (cf. Figures 7, 8, 10a). (b) Conceptual 3-D model of an accommodation zone oblique to the dominant extension direction. The zone is formed by interlocking arrays of oppositely dipping faults and is typically found internally in the analog models and has variable amounts of associated oblique shear (e.g., Figures 8, 9, 10b).

- Nelson, R. A., T. L. Patton, and C. K. Morley, 1992, Rift-segment interaction and its relation to hydrocarbon exploration in continental rift systems: AAPG Bulletin, v. 76, p. 1153–1169.
- Nichol, A., J. J. Walsh, J. Watterson, and P. G. Bretan, 1995, Three-dimensional geometry and growth of conjugate normal faults: Journal of Structural Geology, v. 17, p. 842–862.
- Patton, T. L., A. R. Moustafa, R. A. Nelson, and S. A. Abdine, 1994, Tectonic evolution and structural setting of the Suez rift, in S. M. Landon, ed., Interior rift basins: AAPG Memoir 59, p. 9–56.
- Peacock, D. C. P., and D. J. Sanderson, 1991, Displacement and segment linkage and relay ramps in normal fault zones: Journal of Structural Geology, v. 13, p. 721–733.
- Peacock, D. C. P., and D. J. Sanderson, 1994, Displacements, segment linkage and relay ramps in normal fault zones: AAPG Bulletin, v. 78, p. 147–165.
- Rosendahl, B. R., 1987, Architecture of continental rifts with special reference to East Africa: Annual Review of Earth and Planetary Sciences, v. 15, p. 445–503.
- Rosendahl, B. R., D. Reynolds, P. Lorber, C. Burgess, J. McGill, D. Scott, J. Lambiase, and S. Derksen, 1986, Structural expres-

- sions of rifting: lessons from Lake Tanganyika, in L. E. Frostick et al., eds., Sedimentation in the East African rifts: Geological Society Special Publication 25, p. 29–43.
- Serra, S., and R. A. Nelson, 1989, Clay modelling of rift asymmetry and associated structures: Tectonophysics, v. 153, p. 307–312.
- Tron, V., and J.-P. Brun, 1991, Experiments on oblique rifting in brittle-ductile systems: Tectonophysics, v. 188, p. 71–84.
- Trudgill, B., and J. Cartwright, 1994, Relay-ramp forms and normal-fault linkages, Canyonlands National Park, Utah: Geological Society of America Bulletin, v. 106, p. 1143–1157.
- Walsh, J. J., and J. Watterson, 1991, Geometric and kinematic coherence and scale effects in normal fault systems, in A. M. Roberts, G. Yielding, and B. Freeman, eds., The geometry of normal faults: Geological Society Special Publication 56, p. 193–203.
- Withjack, M. O., and W. R. Jamison, 1986, Deformation produced by oblique rifting: Tectonophysics, v. 126, p. 99–124.
- Younes, A. I., and K. McClay, 2002, Development of accommodation zones in the Gulf of Suez–Red Sea rift, Egypt: AAPG Bulletin, v. 86, no. 6, p. 1003–1026.

